CDF/ANAL/BOTTOM/CDFR/6273
July 24, 2003
Version 2.0

Search for the FCNC decay $D^0 \to \mu^+\mu^-$ using the hadronic B trigger

Bill Ashmanskas
Argonne National Laboratory

Rob Harr
Wayne State University

Abstract

We present a preliminary search for the FCNC decay $D^0 \to \mu^+\mu^-$ using the first 63.5 pb^{-1} of Run II hadronic B trigger data. Using data collected by January 2003 with CDF's SVT-based `B_CHARM` triggers, we expect a sensitivity to $B(D^0 \to \mu^+\mu^-)$, quantified as expected 90% CL limit in the absence of signal, of a few $\times 10^{-6}$. For comparison, the best published limit (at 90% CL) is 4.1×10^{-6}. The Standard Model expectation is 3×10^{-13}, while R-parity violating SUSY models can accomodate a branching ratio as large as 3.5×10^{-6}.

As part of this analysis we investigate the $\pi^\pm$ and $K^\pm$ muon misidentification probabilities. We summarize these results as a function of p_T.

The analysis cuts were optimized with the search window blinded. Optimization yielded an expected background of 1.8 ± 0.7 events. After unblinding, the search window contained no events, resulting in the 90% (95%) confidence level limit of $\mathcal{B}(D^0 \to \mu^+\mu^-) \leq 2.5 \times 10^{-6}$ (3.3×10^{-6}).

1 Motivation

In the Standard Model, the FCNC decay $D^0 \to \mu^+\mu^-$ is suppressed by the GIM mechanism, with a branching ratio estimated [1] to be

$$B_{\mathrm{SM}}(D^0 \to \mu^+\mu^-) \approx 3 \times 10^{-13}. \tag{1.1}$$

(file = fcnc − N.eps)

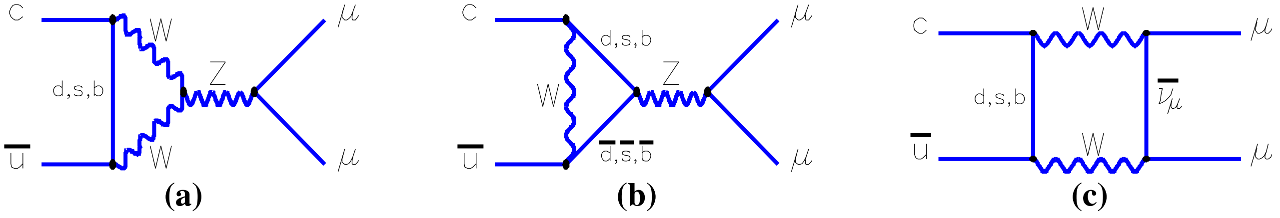

Figure 1: Some one loop contributions to $D^0 \to \mu^+\mu^-$.

(file = rpviol.eps)

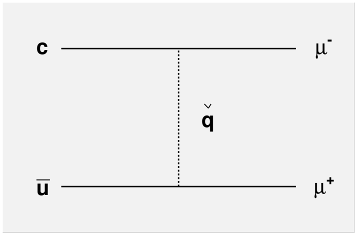

Figure 2: An R-parity violating contribution to $D^0 \to \mu^+\mu^-$.

The GIM cancellation is even more effective for D^0 than for B^0 because the short-distance FCNC amplitude goes like [1] $\sum_{i=d,s,b} V_{ui}V^*_{ci}m_i^2/M_W^2 \sim \lambda(m_s^2 - m_d^2)/M_W^2$ for D^0 versus $\sum_{i=u,c,t} V_{di}V^*_{bi}m_i^2/M_W^2 \sim \lambda^3 m_t^2/M_W^2$ for B^0. (Check this.)

By contrast, some R-parity violating SUSY models can yield $B(D^0 \to \mu^+\mu^-)$ as large as 3.5×10^{-6} [1]. The best published limit, at 90% CL, is 4.1×10^{-6} [2],[3]. Thus, there is a many-decade window in which this decay mode can reveal new physics, to which experiments are just beginning to have sensitivity. In this paper, we show that with data already in hand, CDF may take the lead in this search, edging past the current best experiment. By later this year, we may improve upon the current best search by a factor of four or more. (Important question: What would a limit or observation in this channel mean in terms of masses or couplings?)

B factory $D^0 \to K^-\pi^+$ yields per fb^{-1} are comparable to CDF's yields per pb^{-1}. For example [4], BABAR reconstructed 158K D^*-tagged $D^0 \to K^-\pi^+$ events in 58 fb^{-1}, or 2.7 pb, while CDF reconstructs about 2 nb in this mode. As long as CDF continues to log inverse picobarns at least as fast as BABAR and BELLE log inverse femtobarns, it may maintain the lead in probing this decay mode. Note also that the B factory experiments' muon identification is comparable to CDF's: BELLE quotes an efficiency of 80–85% and a fake rate of 1–2% [5].

2 Analysis strategy

The analysis strategy is as follows:

- Leverage huge SVT fully-reconstructed charm yields [6]
  - $D^0 \to K^-\pi^+ \sim 6$ nb
  - with D^* tag ~ 2 nb
  - $D^0 \to \pi^+\pi^- \sim 210$ pb
  - with D^* tag ~ 70 pb
- Use SVT-triggered $D^0 \to K^-\pi^+$, $D^0 \to \pi^+\pi^-$ samples to understand acceptance, backgrounds, signal normalization
  - The $D^0 \to \mu^+\mu^-$ signal looks basically like $D^0 \to \pi^+\pi^-$ with two muon tags
  - After reducing the combinatoric background below the $D^0 \to \pi^+\pi^-$ signal, the remaining background is expected to be from $D^0 \to \pi^+\pi^-$ with both pions faking muons.

By using a common track-based trigger for both signal and control samples, we can readily normalize to the measured branching ratio $B(D^0 \to \pi^+\pi^-)$, all acceptance effects cancel, and only the relative efficiency for $D^0 \to \pi^+\pi^-$ and $D^0 \to \mu^+\mu^-$ is needed. Thus, the main ingredients needed to make this measurement are

- the number of reconstructed $D^0 \to \pi^+\pi^-$ with both tracks fiducial to the muon detector (for normalization),
- the muon identification efficiency,
- the number of signal events (or an upper limit), based on the number of events observed, and
- the expected background, which can be divided into two parts:
  - $D^0 \to \pi^+\pi^-$ events with both pions misidentified as muons (misidentification), and
  - all other events (combinatoric).

Cuts to remove the combinatoric background can be studied in the high-mass sideband of D^*-tagged $D^0 \to \pi^+\pi^-$ events with zero or one muon tag, and estimated from the double-tagged high-mass sideband. The pion misidentification probability can be determined in D^*-tagged $D^0 \to K^-\pi^+$ events with one or two muon tags, and checked in $D^0 \to \pi^+\pi^-$ events with a single muon identified. In the absence of correlations, the misidentification background can be estimated as the number of $D^0 \to \pi^+\pi^-$ events times the square of the misidentification probability; possible correlations can be studied in the $D^0 \to K^-\pi^+$ sample.

The only element in this analysis that cannot be determined directly from the data is the relative reconstruction efficiency of $D^0 \to \mu^+\mu^-$ to $D^0 \to \pi^+\pi^-$(due to effects such as decay-in-flight, hadronic interactions, etc.). This quantity must be determined from Monte Carlo, but is expected to be close to unity, and will contribute only a small uncertainty to the analysis. The muon identification efficiency, which has been measured by other authors, can be checked directly from the data by using $J/\psi \to \mu\mu$ decays recorded by the μ+SVT or `B_CHARM` trigger.

With all of the pieces in place, we can derive a signal branching ratio,

$$B(D^0 \to \mu\mu) = B(D^0 \to \pi\pi) \times \frac{N(\mu\mu)}{N(\pi\pi)} \times \frac{\epsilon(\pi\pi)}{\epsilon(\mu\mu)} \times \frac{a(\pi\pi)}{a(\mu\mu)}, \tag{2.1}$$

or in the case of an upper limit,

$$B_{90\%\mathrm{CL}}(D^0 \to \mu\mu) = B(D^0 \to \pi\pi) \times \frac{N^{\mathrm{upper}}_{90\%\mathrm{CL}}}{N(\pi\pi)} \times \frac{\epsilon(\pi\pi)}{\epsilon(\mu\mu)} \times \frac{a(\pi\pi)}{a(\mu\mu)}, \tag{2.2}$$

where the N's are the observed numbers of events (or derived limits) in the indicated modes, the ϵ's are the efficiencies for the indicated modes, and the a's are the acceptances for the indicated modes.

3 Monte Carlo studies

We generated and simulated a sample of Monte Carlo events using bgenerator, QQ, svtsim, svtfilter, and the offline reconstruction code, according to the conditions of run 142110, following directions from Alex Cerri. Figure 3 shows the simulated mass spectra. All peaks except $\pi\pi$ are clearly separated from the $\mu\mu$ signal. Even the upper bins of the $K\pi$ signal, 25 times larger than the $\pi\pi$ signal, and with a 60% higher muon double-tag rate, are expected to contribute a negligible background in the signal region: see figure 4.

59% of $\mu\mu$ **tracks** are CMU fiducial; 38% of **pairs**. If we allow CMU or CMX, then 77% of tracks, 59% of pairs, are fiducial. For now, we use CMU.

In Sec. 5 we use the same Monte Carlo, simulating the conditions of run 152747, to estimate the ratio of acceptances and the $\pi\pi$ reconstruction efficiency.

(file = `kkkpipipimumu.ps`)

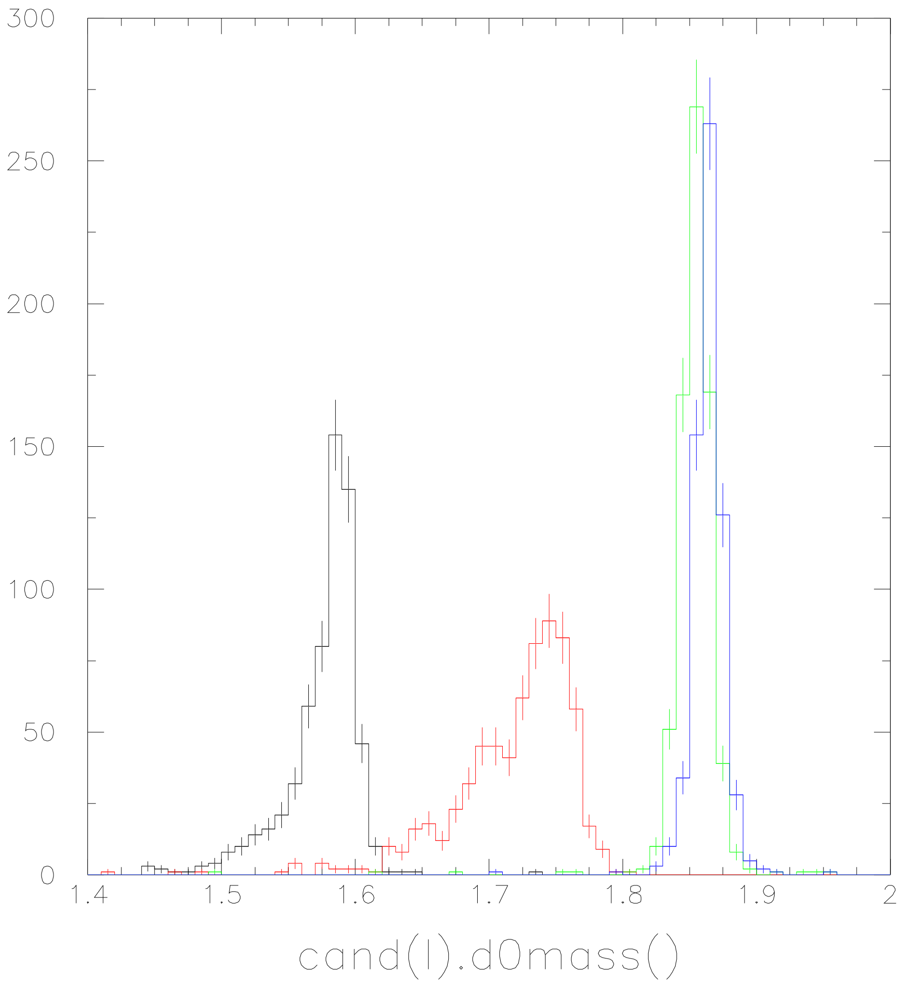

Figure 3: MC mass spectra, using $\mu^+\mu^-$ mass hypothesis, for $D^0 \to KK$, $K\pi$, $\pi\pi$, and $\mu^+\mu^-$.

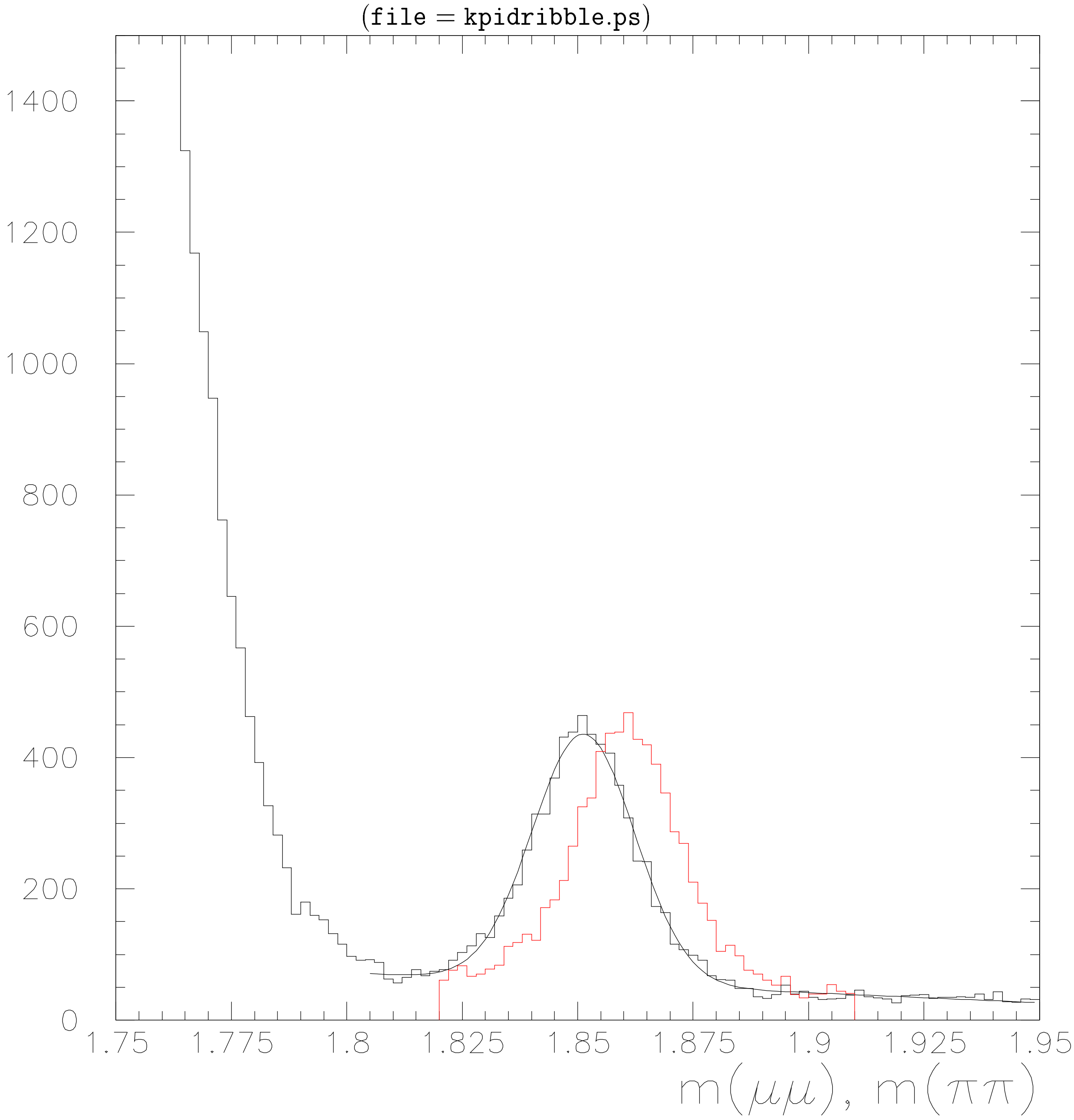

Figure 4: Mass spectrum, from data, of $\pi\pi$ peak and high tail of $K\pi$ signal, using muon mass hypothesis. The $\mu\mu$ signal shape is illustrated in red, by drawing the $\pi\pi$ signal with the pion mass hypothesis.

4 Event selection

We begin with the `hbot0h` CAF data sample, which as of 2003-02-09 contains 2837 files, spanning 761 runs from run 138425 (2002-02-04) to run 156116 (2003-01-05), with a total of 40.3×10^6 events.

We select from this sample events containing loosely defined two-body D^0 decay candidates.

We start from the subset of `defTracks` having `pt` > 0.3 GeV,[(1)] `numCTHitsAx` $\geq$ 25, and `numCTHitsSt` $\geq$ 25. We then look for a matching XFT track satisfying $|\Delta\frac{1}{p_T}| < 8\%/\mathrm{GeV}$, $|\Delta\phi(r = 105.575\ \mathrm{cm})| < 0.015$.[(2)] If an XFT match is found, we look for the SVT track (if any) that is linked to that XFT track.[(3)]

To form D^0 candidates, we loop over pairs of SVT-matched tracks, requiring $|d_{\mathrm{SVT}}| \geq 0.0100$ cm,[(4)] $d^i_{\mathrm{SVT}} \cdot d^j_{\mathrm{SVT}} < 0$, $c^i \cdot c^j < 0$. We use `VertexFit` (a.k.a. `CTVMFT`) to intersect the tracks. We only require the fit not to fail, so that we can calculate track momenta at the point of intersection; there is no χ^2 requirement. The invariant mass of the candidate, using the muon mass hypothesis, must satisfy $1.50 \leq m \leq 2.05$ GeV. Figure 3 shows that this window is wide enough to be fully efficient for collecting $K\pi$, $\pi\pi$, and $\mu\mu$ candidates. This procedure selects 3.43×10^6 events, which we write out to a binary micro-DST.

We next try (still within `AC++`) to match each D^0 candiate with "bachelor" pions to form D^{*+} candidates. Bachelor pion tracks are not required to pass the XFT/SVT match requirements, since their typical momentum is $\sim 0.140 * 5.5/1.865 \approx 0.4$ GeV. We use `VertexFit` again, this time requiring the D^0 pseudotrack to intersect the soft pion track, and require $m_{D^*} - m_{D^0} \leq 0.17$ GeV.[(5)]

If at this point we require $0.144 < m_{D^*} - m_{D^0} < 0.147$ GeV, using the $K\pi$ mass assignment, we see 140K $D^0 \to K^-\pi^+$ candidates (fitting `P1+G+G`). The window $0.144 < m_{D^*} - m_{D^0} < 0.147$ GeV is justified by figure 13 for $D^0 \to K^-\pi^+$ and by figure 6 for $D^0 \to \pi^+\pi^-$.

At the ntuple level, we apply several additional track-quality and trigger-confirmation cuts. For each of the two D^0 daughters, we require $p_T > 2$ GeV, $0.0120\ \mathrm{cm} \leq |d_{\mathrm{SVT}}| \leq 0.1000$ cm, and that the offline track use hits in at least three SVXII axial layers. We require that the track pair satisfy $2^\circ < |\Delta\phi| < 90^\circ$ and $L_{xy} > 0$. After these cuts, we see 137K D^*-tagged $D^0 \to K^-\pi^+$ candidates (fitting

---

(1) In practice, offline tracks having $p_T < 1.33$ GeV are never matched to XFT tracks.

(2) In case of > 1 match, we use the XFT track minimizing $(\Delta\frac{1}{p_T}/(1.6\%/\mathrm{GeV}))^2 + (\Delta\phi/0.0022)^2$.

(3) Each SVT track records its XFT parent ID, and the SVT GhostBuster board ensures that at most one SVT track is linked to a given XFT track.

(4) By the ntuple stage, fewer than 0.3% of candidate tracks have $|d_{\mathrm{SVT}}| < 0.0120$ cm

(5) The Δm cut is made very loose at this stage because we use the muon mass hypothesis for the D^0 decay daughters, but want to be efficient for $K\pi$ and $\pi\pi$.

P1+G+G), having $0.144 < m_{D^*} - m_{D^0} < 0.147$, as shown in figure 5.

Note that we make no use of offline impact parameter information, except in the calculation of the point of intersection at which track momenta are evaluated.

We select good runs by querying the offline production database. We require $138425 \leq$ RUNNUMBER ≤ 156116 and that the following flags have the value '1': RUNCONTROL_STATUS, SHIFTCREW_STATUS, CLC_STATUS, SVX_STATUS, SVT_STATUS, L1T_STATUS, L2T_STATUS, L3T_STATUS, OFFLINE_STATUS, COT_OFFLINE, CMU_OFFLINE. This yields 440 runs, 63.549 pb^{-1}. We checked that for every one of these 440 runs, there is at least one D^*-tagged $D^0 \to K^-\pi^+$ candidate in our ntuple. We also checked the effective D^*-tagged $D^0 \to K^-\pi^+$ cross-section vs run number: see figure 8.(6) As a final check, we relax the SVX_STATUS and SVT_STATUS requirements but require $138425 \leq$ RUNNUMBER ≤ 152625. We verify that we can reproduce the luminosity calculation of CDF 6288: 458 runs, 39.096/pb.

We next fit the $D^0 \to \pi^+\pi^-$ normalization signal. Using the $\mu\mu$ mass hypothesis, we find (fitting P1+G) 4345 ± 90 events with a gaussian peak position of 1.851 GeV and $\sigma = 11$ MeV, and using the $\pi\pi$ mass hypothesis, we find the same number of events with a peak at 1.861 GeV and $\sigma = 11$ MeV (figure 9). So a $\pm 2\sigma$ search window for the signal would span $1.839 < m < 1.883$ GeV. Because the signal and background peaks are separated by $\approx 1\sigma$, it would make sense to optimize the lower and upper edges of the search window separately. For now, however, we have made the ad-hoc choice of a $\pm 2\sigma$ window.

After the muon fiducial cut, described in section 5, the $K\pi$ and $\pi\pi$ yields are reduced, by a factor of roughly 0.36, to 41500 ± 400 and 1583 ± 60 events, respectively (figure 10).

We will apply a few final cuts, to optimize search sensitivity, in section 7.

5 Relative efficiency

One factor in our search sensitivity is the ratio of efficiencies for the $\mu\mu$ signal and the $\pi\pi$ normalization mode. We require both muon signal candidate tracks and pion normalization candidate tracks to be fiducial in the CMU.(7) We tag tracks as muon candidates if they are associated with CMU stubs.(8)

The efficiency for detecting a muon stub was explored by Bloom and Dagenhart in CDF 6029 [8] by using the unbiased muon in $J/\psi \to \mu\mu$ candidates found in the μ+SVT trigger sample. The analysis of 6029 finds the ratio of the fraction of

(6) Note the anomalous behavior of run 151811: it has a LUMI_LIVE value of 20.5/nb, but multiplying the livetime by the average instantaneous luminosity gives 88/nb.

(7) `MuonFiducialTool::isFiducial(muon,MuonDigiCode::CMU)`

(8) `muon->hasCmu()` and `muon->cmu().chsqXPosition()<=9`

(file = mkpiallruns.ps)

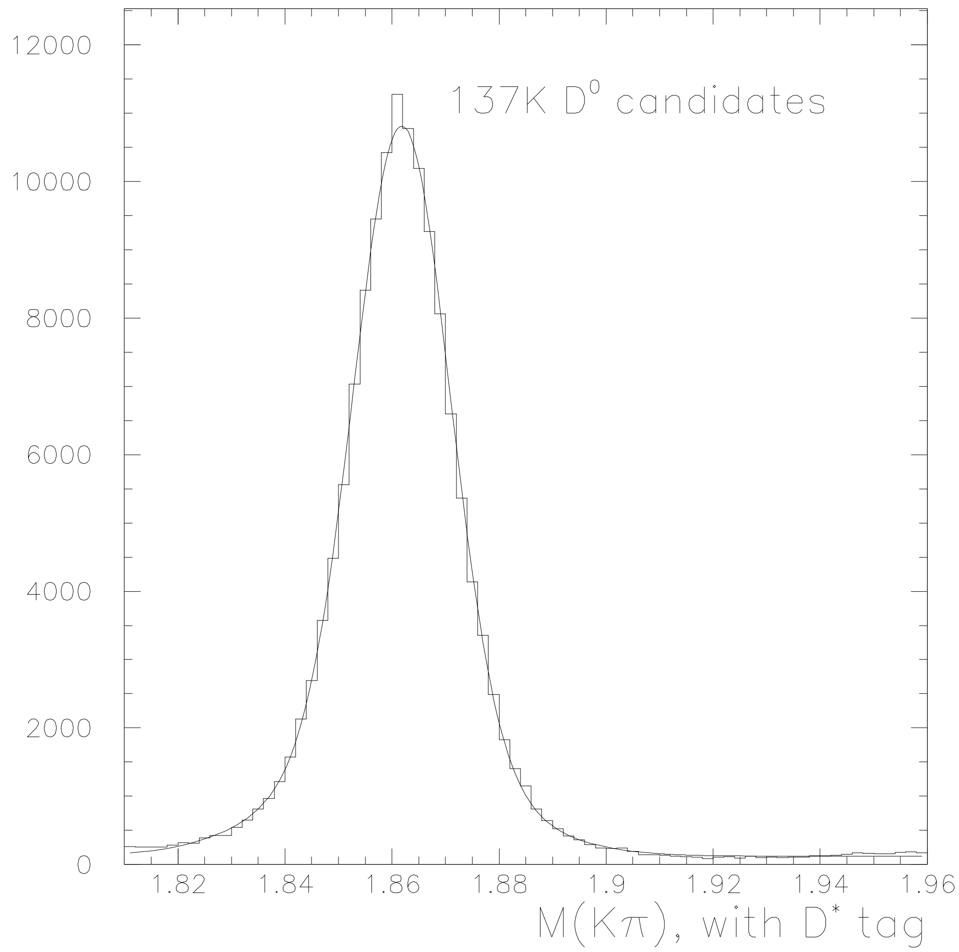

Figure 5: Mass spectrum of D^*-tagged $D^0 \to K\pi$ candidates, after basic track-quality and trigger-confirmation cuts, but before good run requirement, final clean-up cuts, or muon fiducial requirement.

(file = dstarpipi.ps)

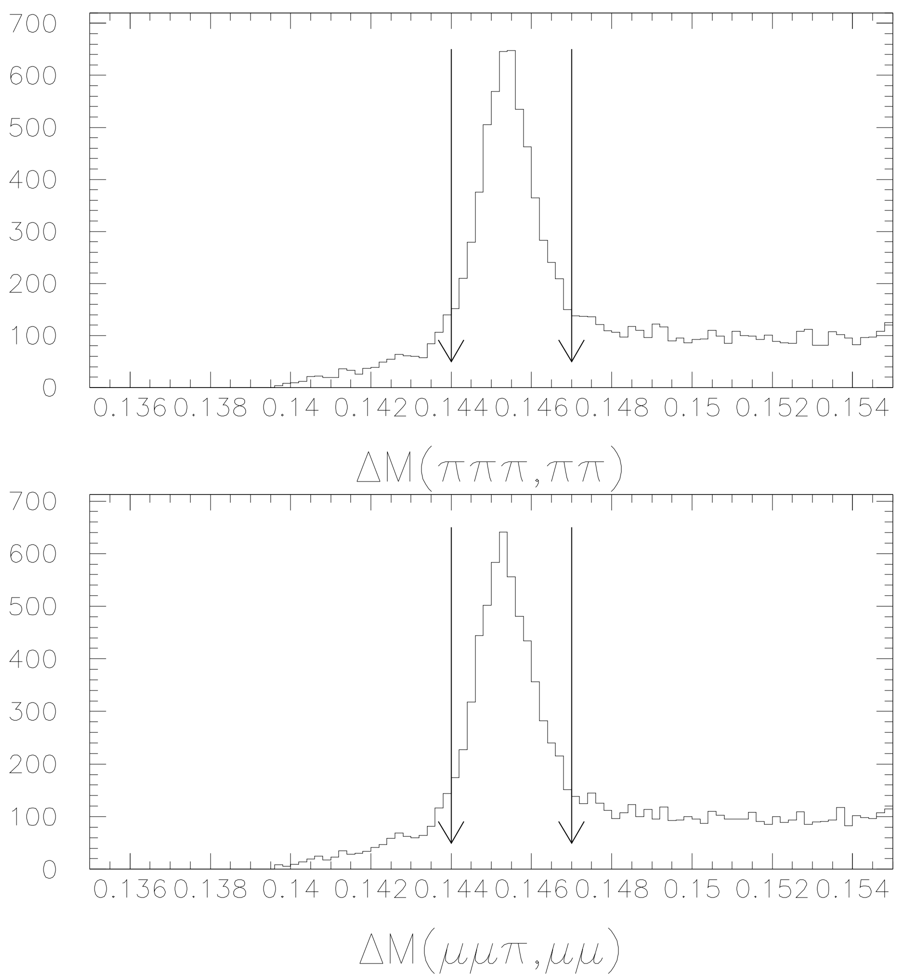

Figure 6: Justification of $0.144 < m_{D^*} - m_{D^0} < 0.147$ GeV window, for $\pi\pi$ and $\mu\mu$ mass hypotheses, for $1.83 < m_{\pi\pi} < 1.89$ GeV. The difference between $\pi\pi$ and $\mu\mu$ mass hypotheses is negligible for the Δm distributions. This is important, since we use the $\pi\pi$ signal to normalize the $\mu\mu$ search. The exact boundaries of this window could be optimized to maximize search sensitivity, but at this point have been chosen by eye.

(file = mkpigoodrun.ps)

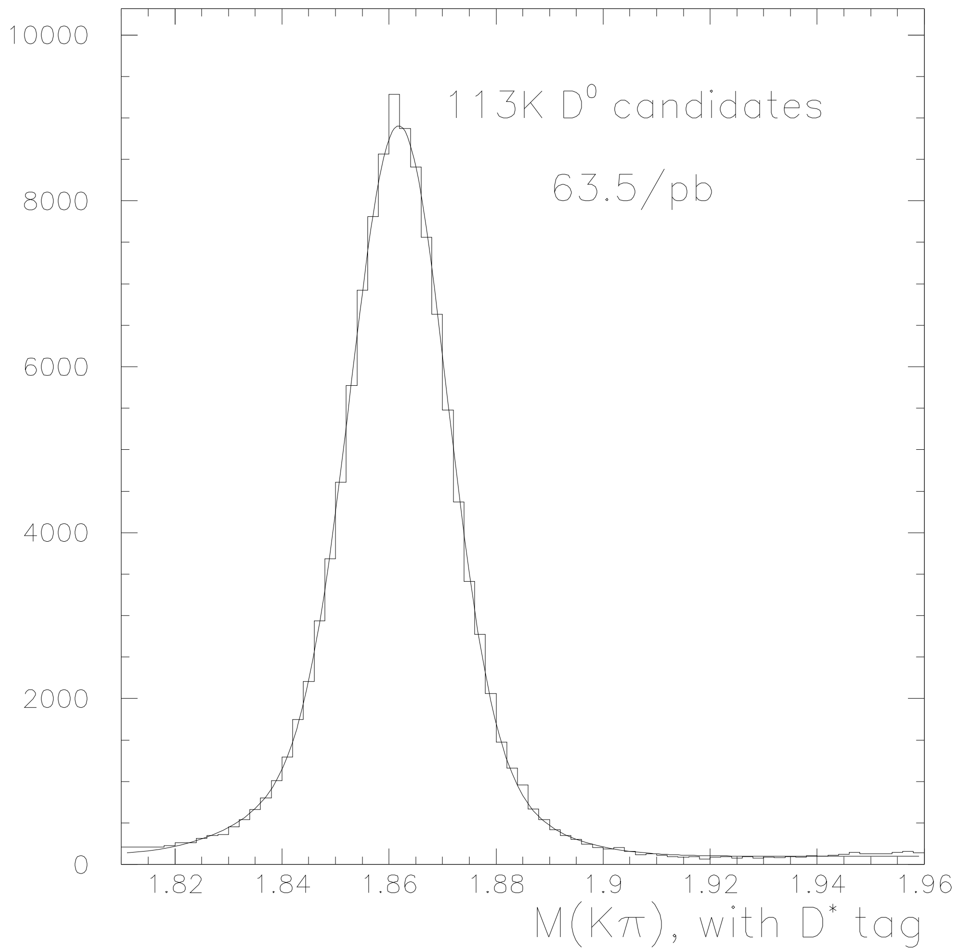

Figure 7: Mass spectrum of D^*-tagged $D^0 \to K\pi$ candidates, after basic track-quality and trigger-confirmation cuts, after good run requirement, but before final clean-up cuts, or muon fiducial requirement.

(file = xsecvsrun.ps)

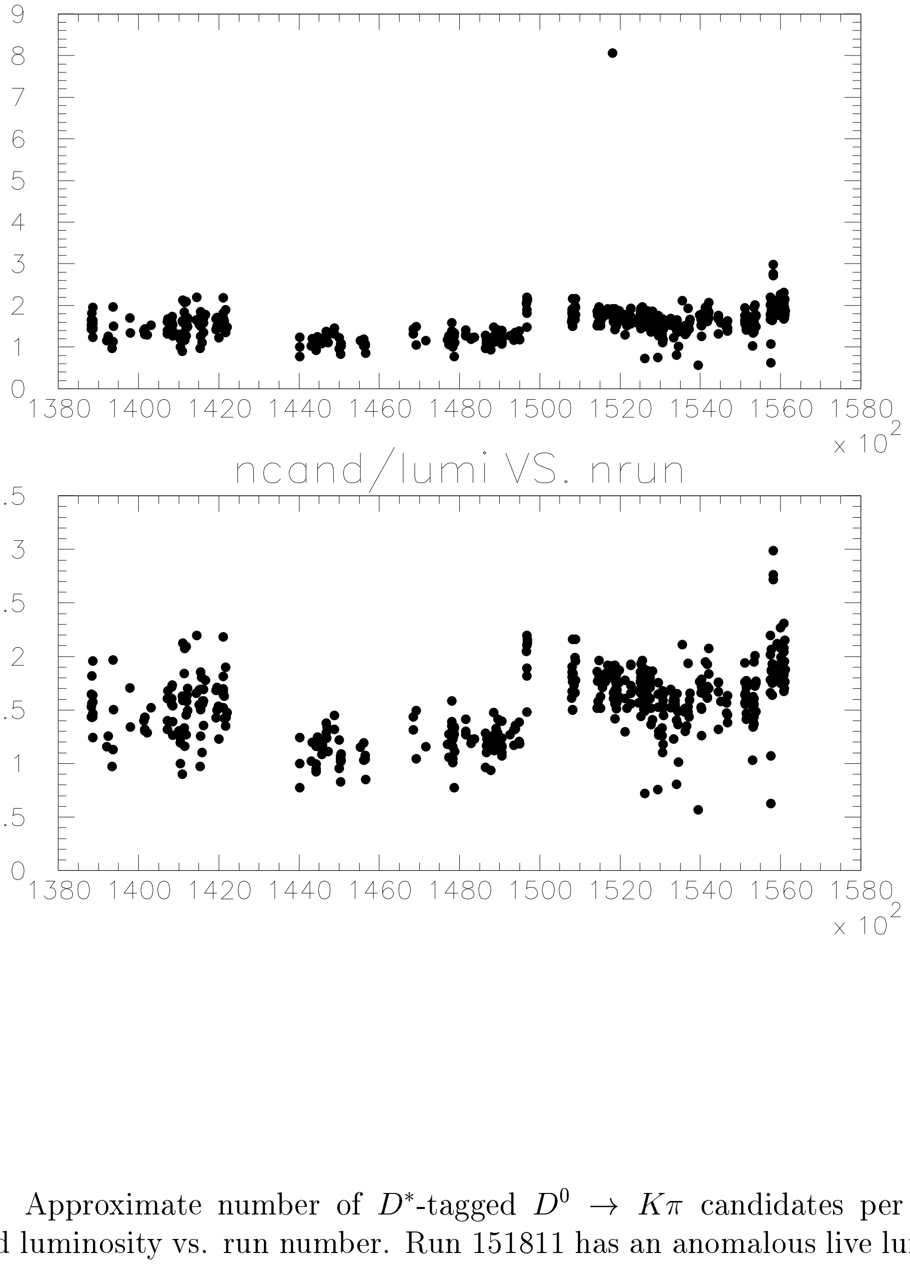

Figure 8: Approximate number of D^*-tagged $D^0 \to K\pi$ candidates per nb^{-1} of integrated luminosity vs. run number. Run 151811 has an anomalous live luminosity in the database. In runs 155818–155821, SVT used "4/5" majority logic.

(file = mmumumpipi.ps)

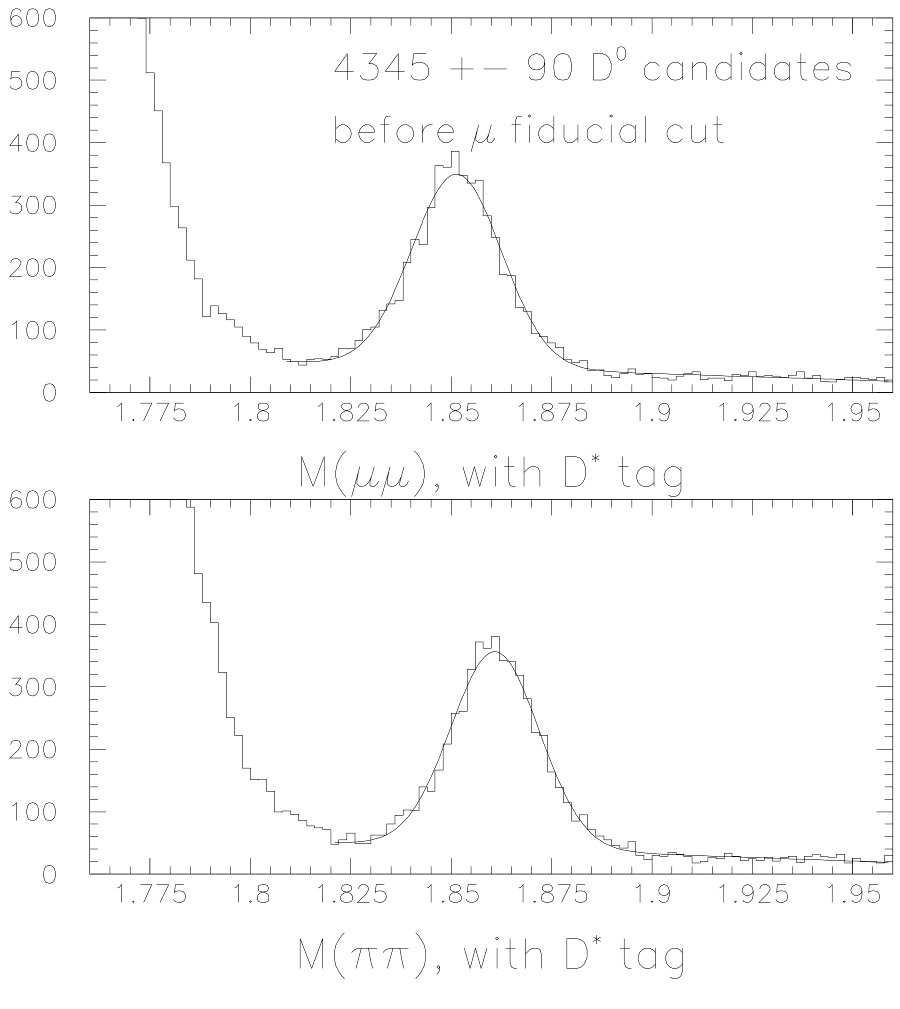

Figure 9: $\mu\mu$ and $\pi\pi$ mass spectra, with D^* tag, before muon fiducial cuts.

(file = mmumumkpicmufid.ps)

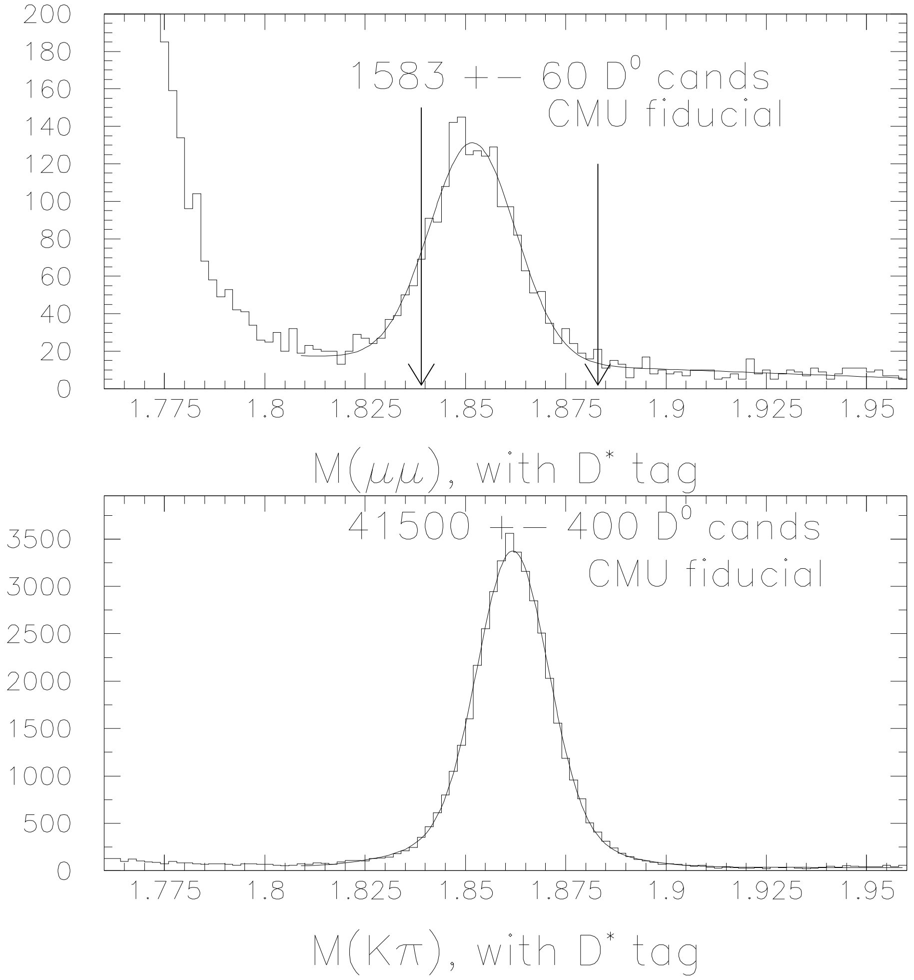

Figure 10: $\mu\mu$ and $K\pi$ mass spectra, with D^* tag, after muon fiducial cuts. The top peak is fit with `P1+G`, and the bottom peak with `P1+G+G`. The arrows in the top plot indicate the $\mu\mu$ signal search window. The event counts are the full areas of the gaussian fits.

unbiased muon tracks passing the CMU `isFiducial` requirement and are matched with a muon stub in data relative to the fraction in Monte Carlo. In the $D^0 \to \mu^+\mu^-$ measurement, we need the raw efficiency without the Monte Carlo correction. Also, we use a 0, cm fiducial cut as opposed to the -10 cm fiducial cut used in 6029. Bloom and Dagenhart still had their ntuple available and were able to run through it to produce a muon efficiency result appropriate for use in this measurement. The muon identification efficiency as a function of p_T (Fig. 11) is convoluted with the spectra of p_T in $D^0 \to \pi^+\pi^-$ decays (Fig. 12) to yield a dimuon detection efficiency of 0.80 ± 0.03. In future updates of this analysis, we plan to repeat the μ+SVT checks ourselves, where we can explore how to best optimize the fiducial requirements.

CDF 6018 [6] finds a $4.5 \pm 0.2\%$ probability for a pion to interact hadronically or decay with a resulting loss of the track in reconstruction. About 4% of the loss is from hadronic interactoins and 0.5% from decays-in-flight. The quoted error is statistical only. The authors of 6018 estimate a 1% systematic error due to differences between the FLUKA and GEISHA packages for simulating hadronic interactions. We checked these results with the Monte Carlo discussed in Sec. 3, comparing the yield of $\pi\pi$ events with and without decays-in-flight and hadronic interactions. The result is a $\pi\pi$ reconstruction efficiency of $\epsilon(\pi\pi) = 0.90 \pm 0.02$.

Combining the above ingredients, we estimate $\epsilon_{\pi\pi}/\epsilon_{\mu\mu} = 1.13 \pm 0.04$.

Using the same Monte Carlo as above, we determined the ratio of acceptances and found $a(\pi\pi)/a(\mu\mu) = 0.96 \pm 0.02$. This result can be compared to the equivalent ratios for KK, $K\pi$, and $\pi\pi$ decays presented in CDF 6018. They find the ratios $a(K\pi)/a(KK) = 1.07 \pm 0.03$ and $a(K\pi)/a(\pi\pi) = 0.98 \pm 0.03$. (In the note, ϵ is used in place of a.) The result $a(\pi\pi)/a(\mu\mu) = 0.96 \pm 0.02$ is consistent with CDF 6018.

Note that we avoid catastrophic blunders, such as running with the muon chambers switched off, by including the `CMU_OFFLINE` good run bit in the event selection. Two additional checks that we intend to perform in the future are to estimate the J/ψ cross-section for each run used in the search and to graph the $K \to \mu$ fake rate as a function of date, to make sure both are relatively flat.

Finally, we need to consider correlated inefficiencies in muon identification. One example of an efficiency loophole is our trigger sample's lack of any requirement on the distance between track pairs when swum to the muon chambers, compared with CDF 6288's J/ψ sample's trigger requirement that the muons be separated by at least ????? (a stack? a wedge?). One of the final clean-up cuts that we describe in section 7 requires that the D^0 decay daughters be separated by at least about 4.5 CMU drift cells.(9) This cut is expected to eliminate the most obvious source of correlated inefficiency, but we ought to make more checks in the μ+SVT sample.

(9) The CMU cell size (full width) is about 6.35 cm. The chambers are at a radius of about 347 cm. The separation cut we use is 85mrad.

(file = $\mathtt{mu_eff.eps}$)

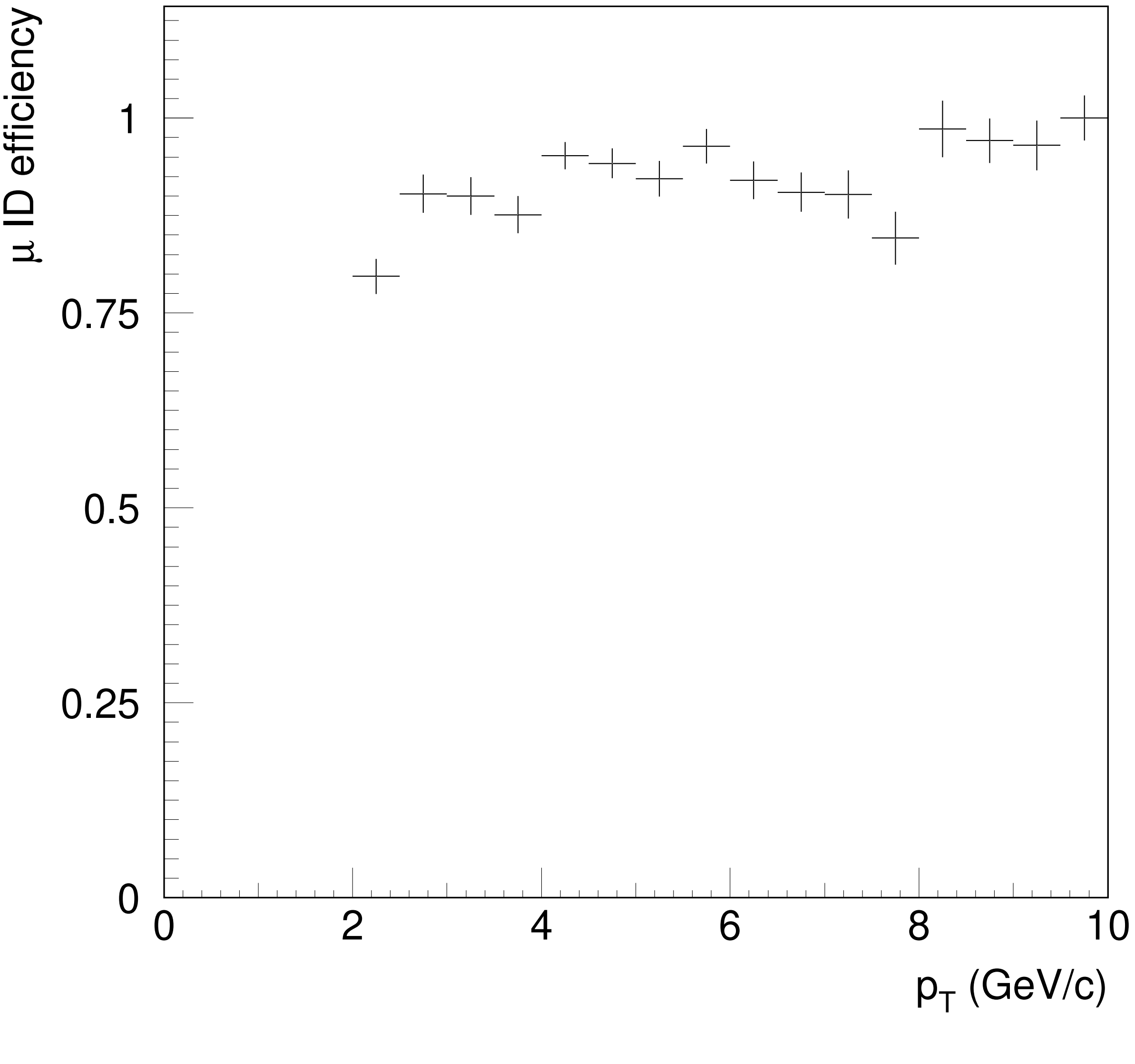

Figure 11: The muon identification efficiency as a function of p_T of the track. The efficiency is determined following the procedure described in CDF 6029 with the modifications discussed in the text.

(file = pt1pt2.eps)

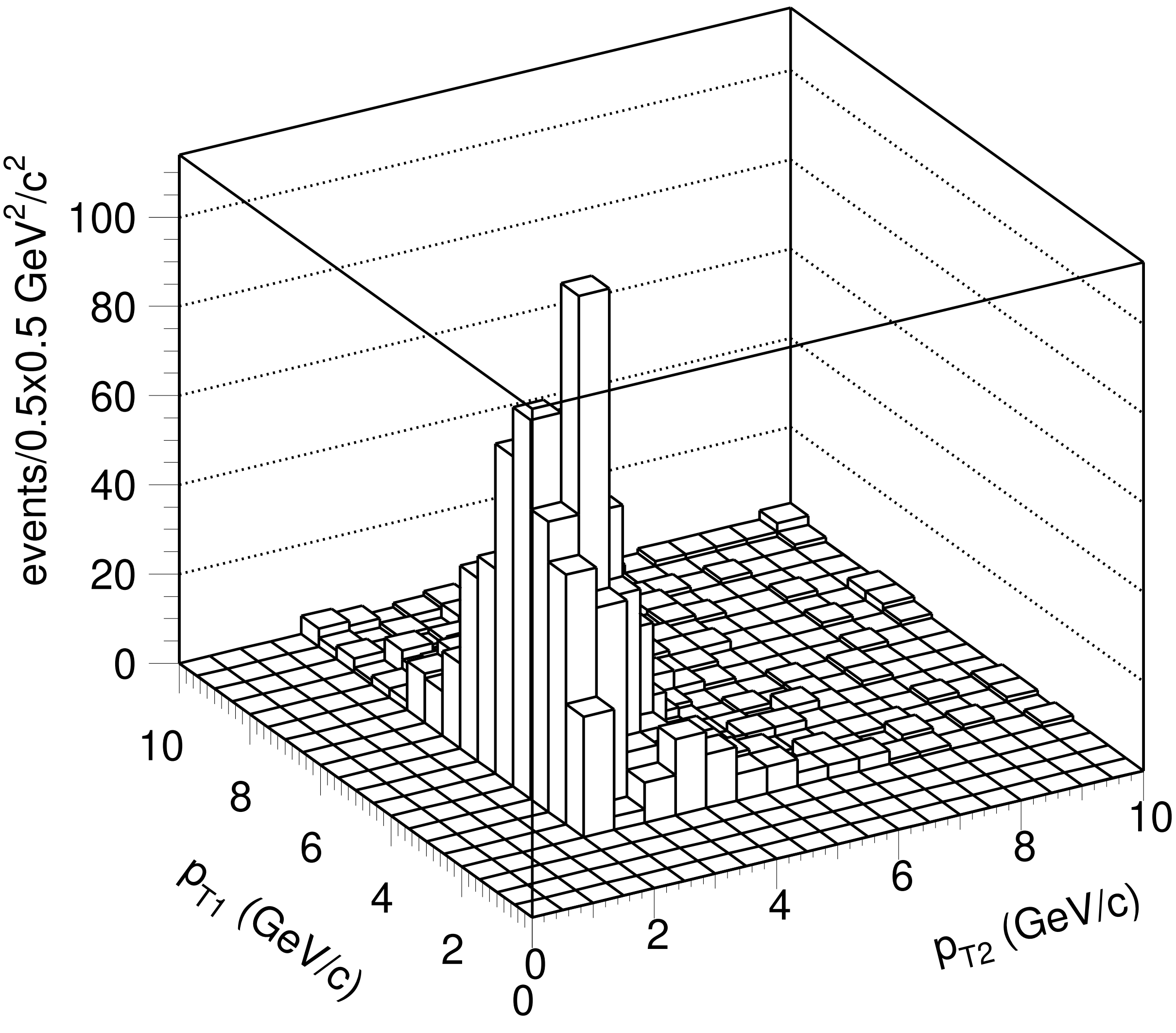

Figure 12: The frequency of the combination of p_T's for the pions in $D^0 \to \pi^+\pi^-$ candidates. Usually $p_{T1} \geq p_{T2}$ but this condition is not rigorously enforced.

6 π and K misidentification as muons

One of the background contributions to $D^0 \to \mu^+\mu^-$ is from $D^0 \to \pi^+\pi^-$ events with both pions misidentified as muons. To make an estimate of this background we look at the probability for the pion track in $D^0 \to K^-\pi^+$ decays to be assigned to a muon stub. By matching a tagging pion with the D^0 pseudotrack and applying $D^{*\pm}$ selection criteria (Fig. 13), we reduce the background events (Fig. 14) and, neglecting the doubly-cabibo-suppressed decays, determine the kaon and pion mass assignments based on the charge of the tagging pion.

We divide the data into p_T bins for each of π^+, π^-, K^+, and K^-, as shown in Figures 15, 17, 19, and 21, respectively, requiring both tracks to be fiducial to the CMU. While the kaon misidentification probability is not required in this analysis, it is almost no additional work to obtain the result. For each histogram, we determine the background subtracted signal, where the bins shaded red represent signal, and the sidebands in blue are background. Call these quantitities $n_i(p_T)$ for particle type i.

Those events where the selected track is associated with a muon stub are plotted in Figures 16, 18, 20, and 22. Agan we determine the background subtracted signal, call these $m_i(p_T)$.

Finally, for each p_T bin the misidentification probability for particle species i is given by:

$$\mathcal{P}_{i \to \mu}(p_T) = \frac{m_i(p_T)}{n_i(p_T)} \ . \tag{6.1}$$

The result is displayed in Figure 23 for $\pi^\pm$ and Figure 24 for $K^\pm$, and listed in Table 1. The pion misidentification probability is roughly the same for each charge, as expected, while the misidentification probability for K^+ is about twice that for K^-. This can be understood from the higher interaction cross section of $K^-$with protons and neutrons, making it less likely than K^+ to pass through the calorimeter and muon abosorber without interacting.

7 Background estimate and cut optimization

Using the pion misidentification calculation described in Sec. 6, we find that (folded with the track p_T spectra) 2.4% of CMU-fiducial kaons and 1.4% of CMU-fiducial pions are matched with CMU stubs.

Naively, we might read from figure 10 that we expect, before muon tagging, $\approx 0.84 \times 1583 = 1330$ resonant and $\approx 20 \times 0.044/0.002 = 440$ combinatorial background events in the $\mu\mu$ signal window. If every background track is a pion, we might expect (file = dstar$_{\text{k}}$pi.eps)

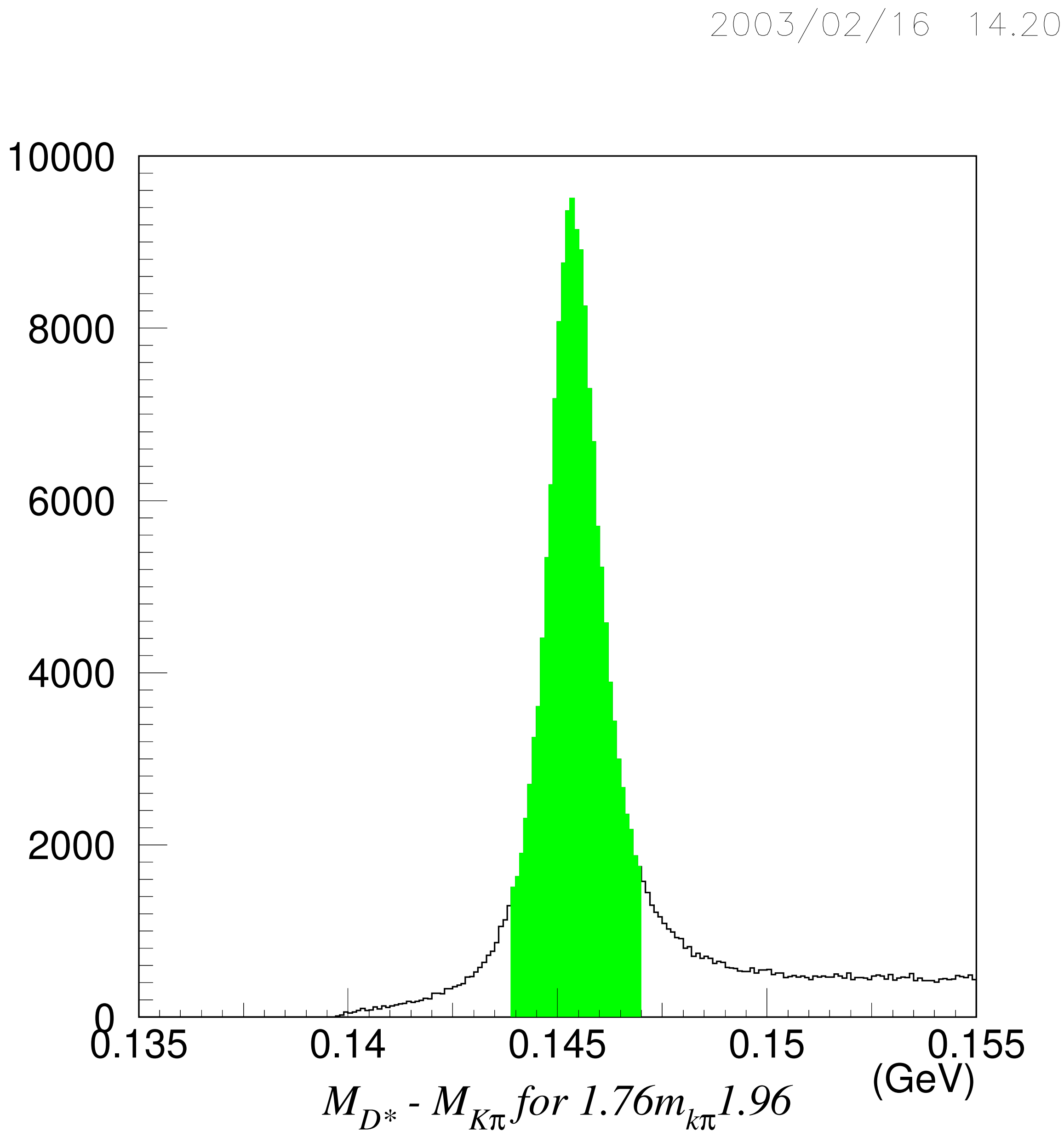

Figure 13: The distribution of $M(\pi_{D^{*\pm}}K\pi) - M(K\pi)$ mass difference based on the full winter 2003 data set. The shaded region indicates the events selected by the $D^{*\pm}$ tag.

(file = mkpi$_d$star.eps)

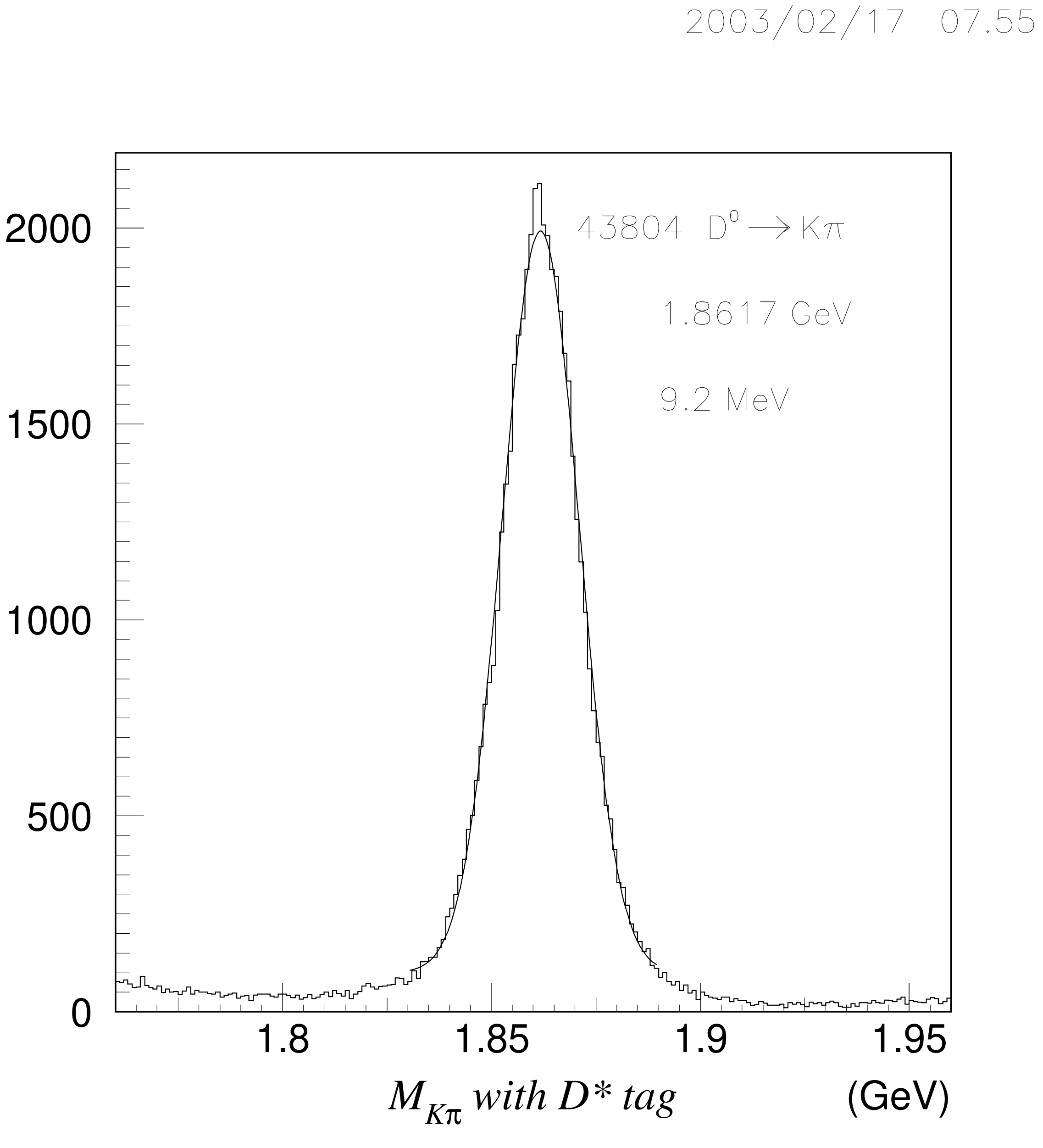

Figure 14: $K\pi$ mass spectrum with $D^{*\pm}$ selection and track fiducial requirement for the winter 2003 data. The peak is fit to a gaussian plus constant background term, and the integral of the gaussian fit is displayed.

(file = $\mathtt{mkpi_p ip_p t.eps}$)

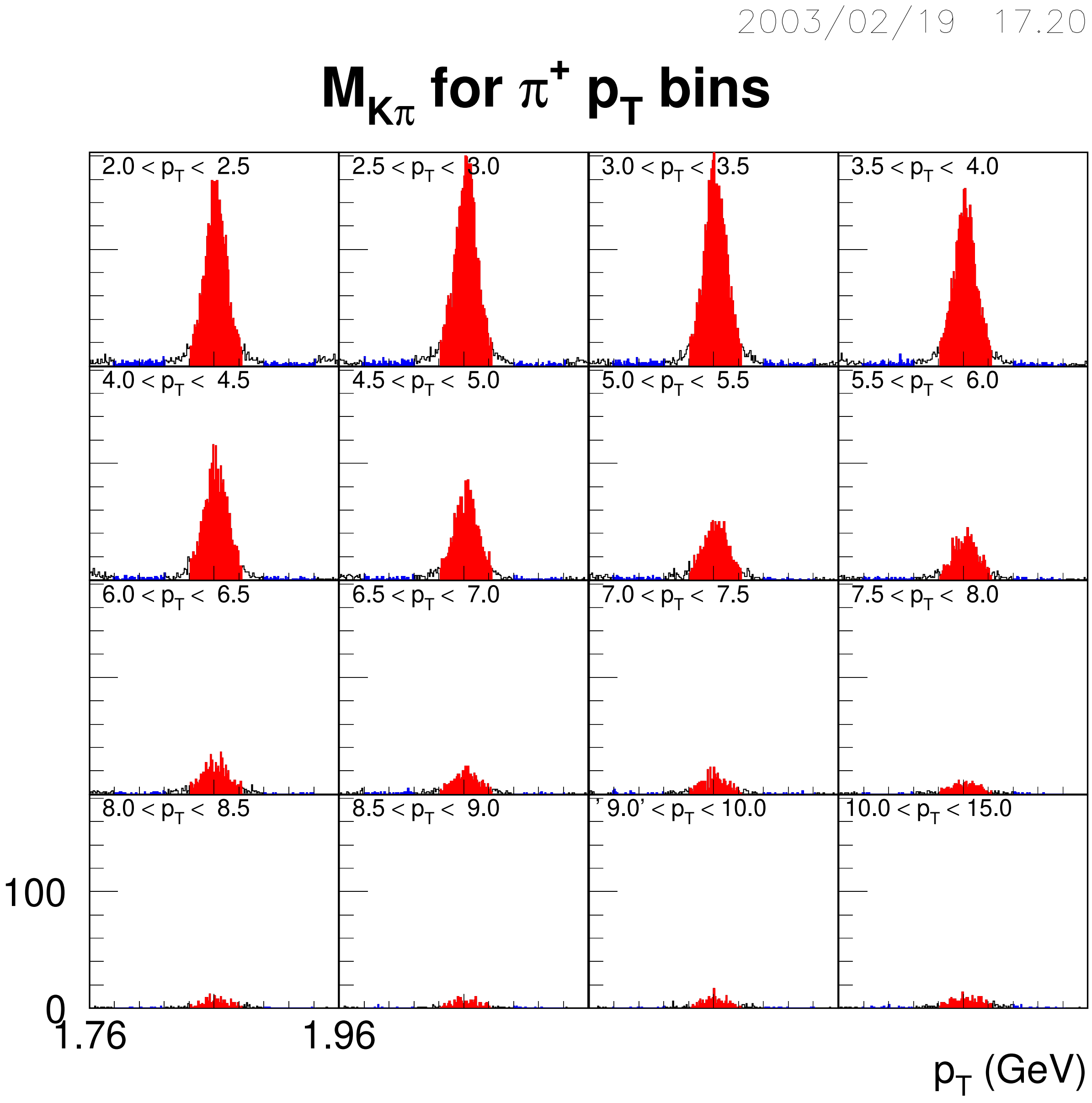

Figure 15: $K^-\pi^+$ mass spectra, binned by p_T of the pion.

$(\texttt{file} = \texttt{mkpi}_\texttt{p}\texttt{ip}_\texttt{p}\texttt{t}_\texttt{m}\texttt{uid.eps})$

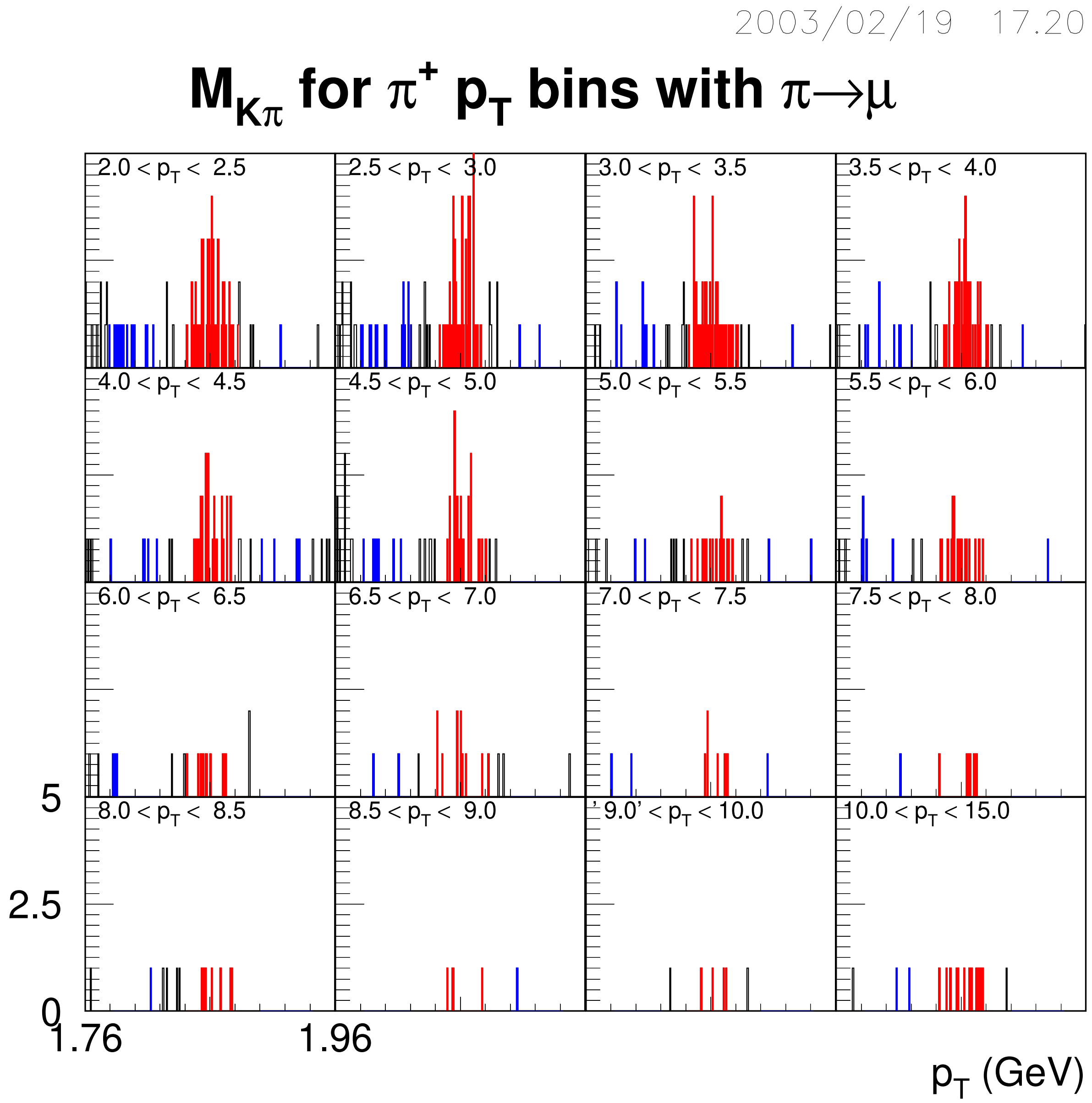

Figure 16: $K^-\pi^+$ mass spectra for pions matched to a muon stub, binned by p_T of the pion.

(file = $\mathtt{mkpi_pim_pt.eps}$)

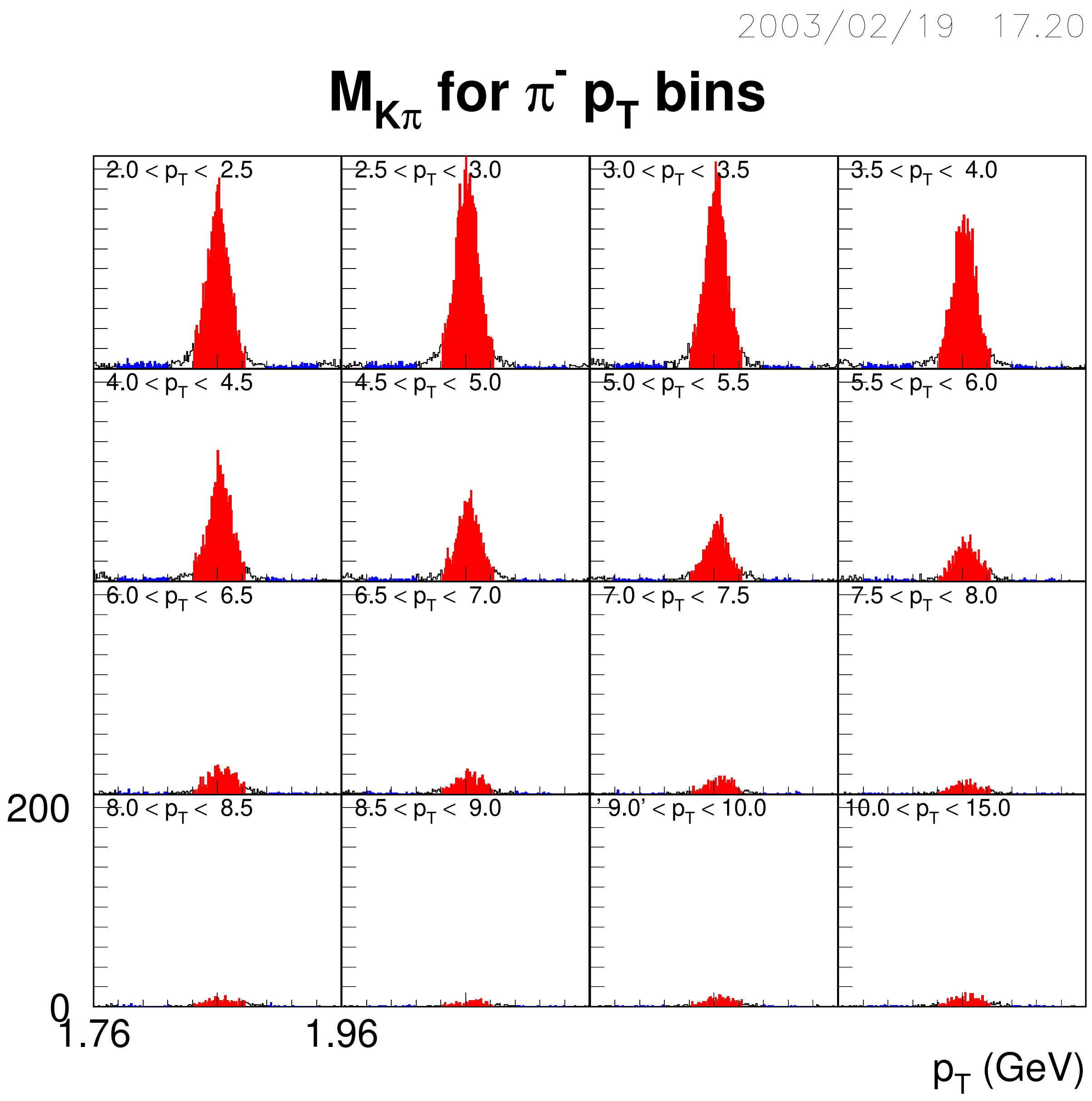

Figure 17: $K^+\pi^-$ mass spectra binned, by p_T of the pion.

(file = mkpi_pim_pt_muid.eps)

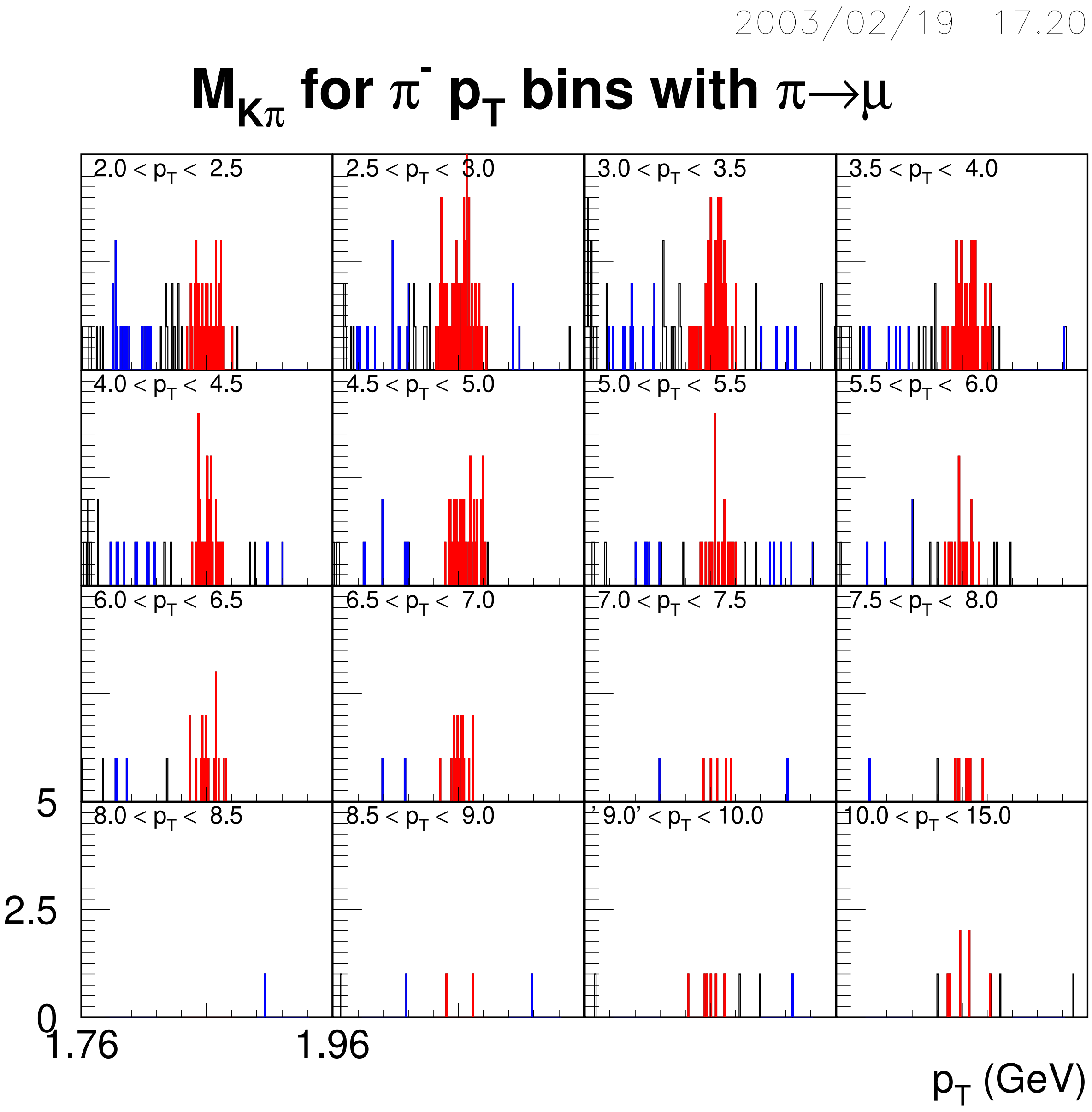

Figure 18: $K^+\pi^-$ mass spectra for pions matched to a muon stub, binned by p_T of the pion.

(file = mkpi_kp_pt.eps)

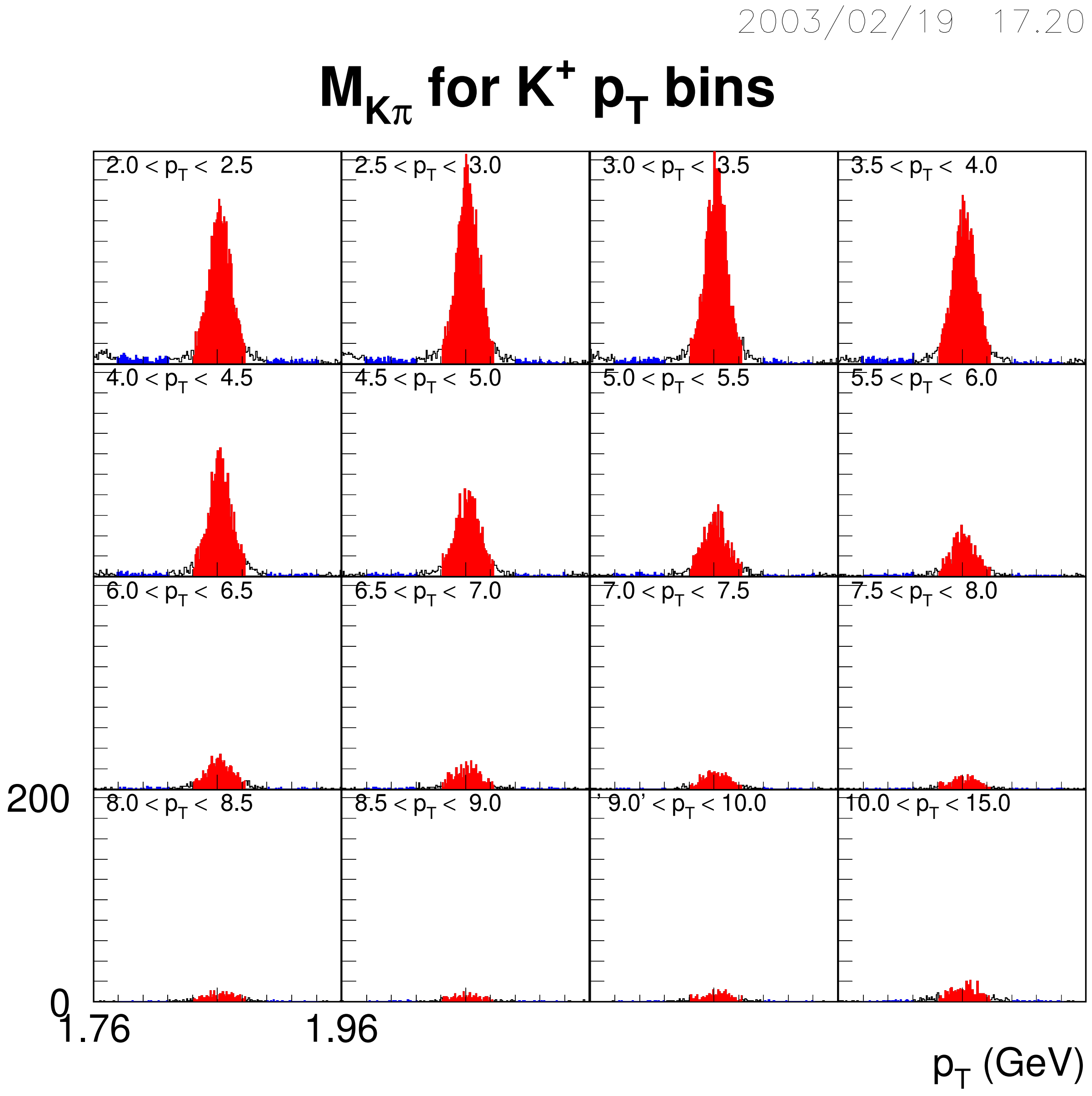

Figure 19: $K^+\pi^-$ mass spectra binned, by p_T of the kaon.

(file = $\mathtt{mkpi_k p_p t_m uid.eps}$)

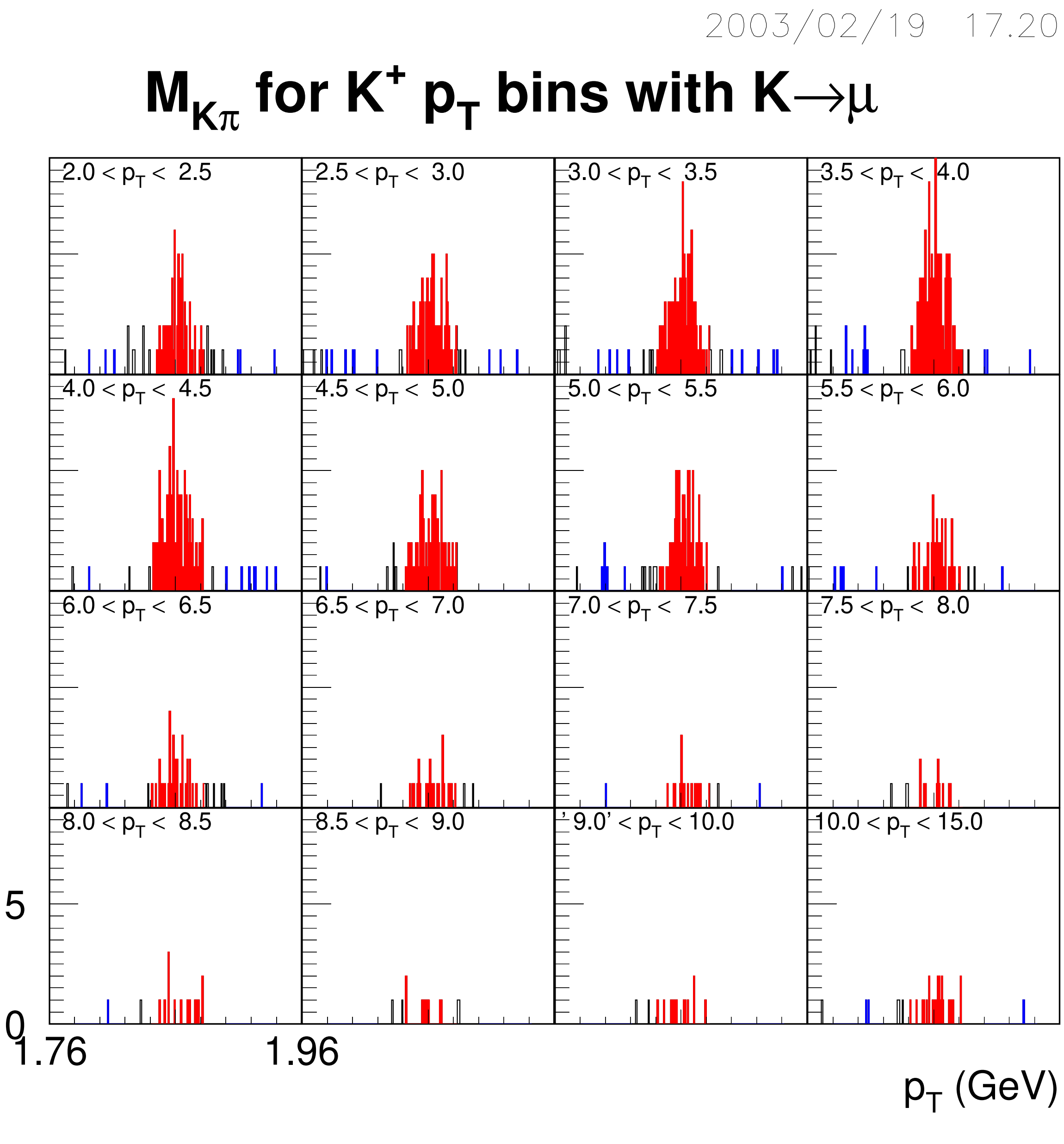

Figure 20: $K^+\pi^-$ mass spectra for kaons matched to a muon stub, binned by p_T of the kaon.

(file = mkpi_k m_p t.eps)

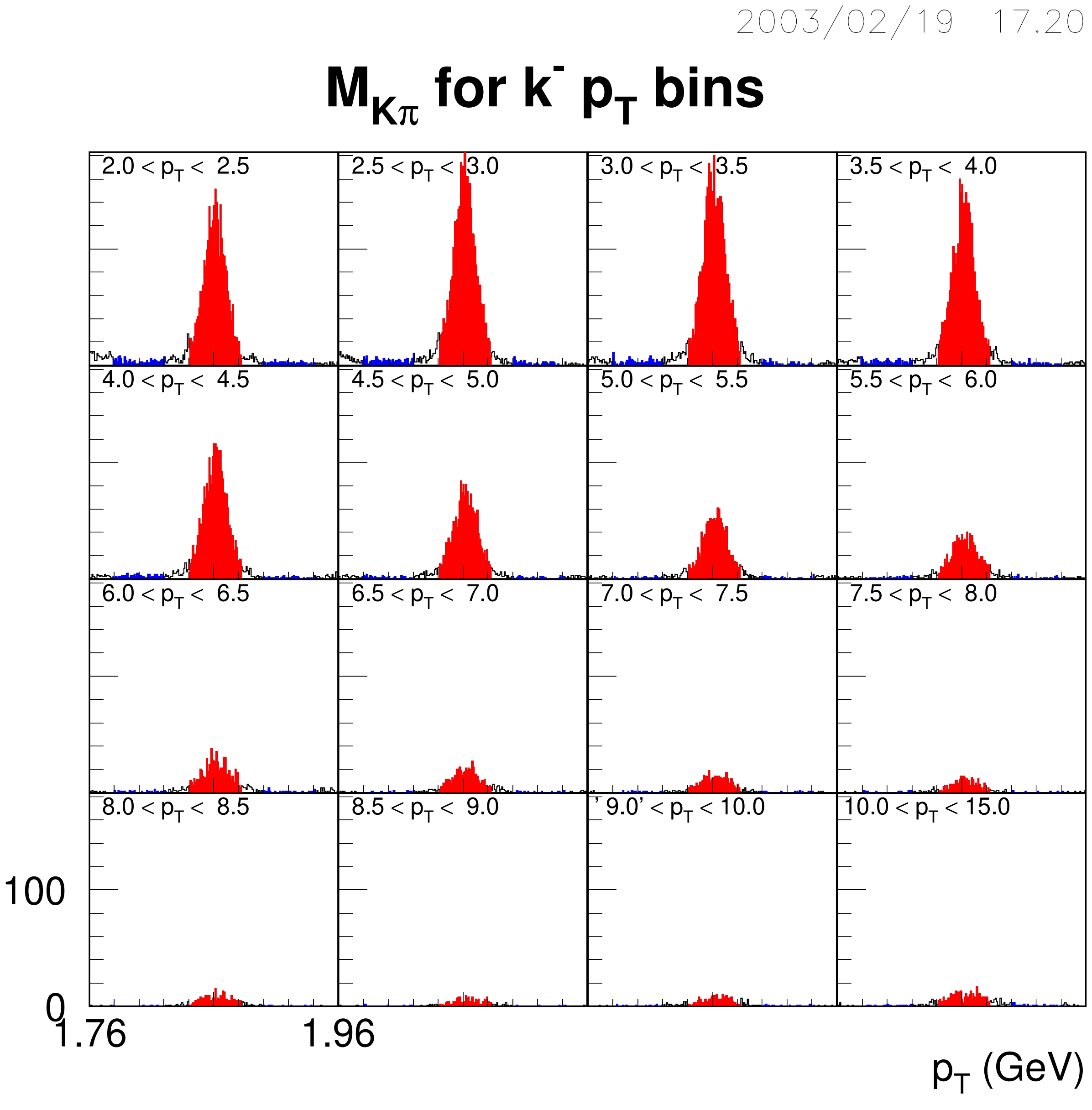

Figure 21: $K^-\pi^+$ mass spectra binned, by p_T of the kaon.

(file = mkpi_k m_p t_m uid.eps)

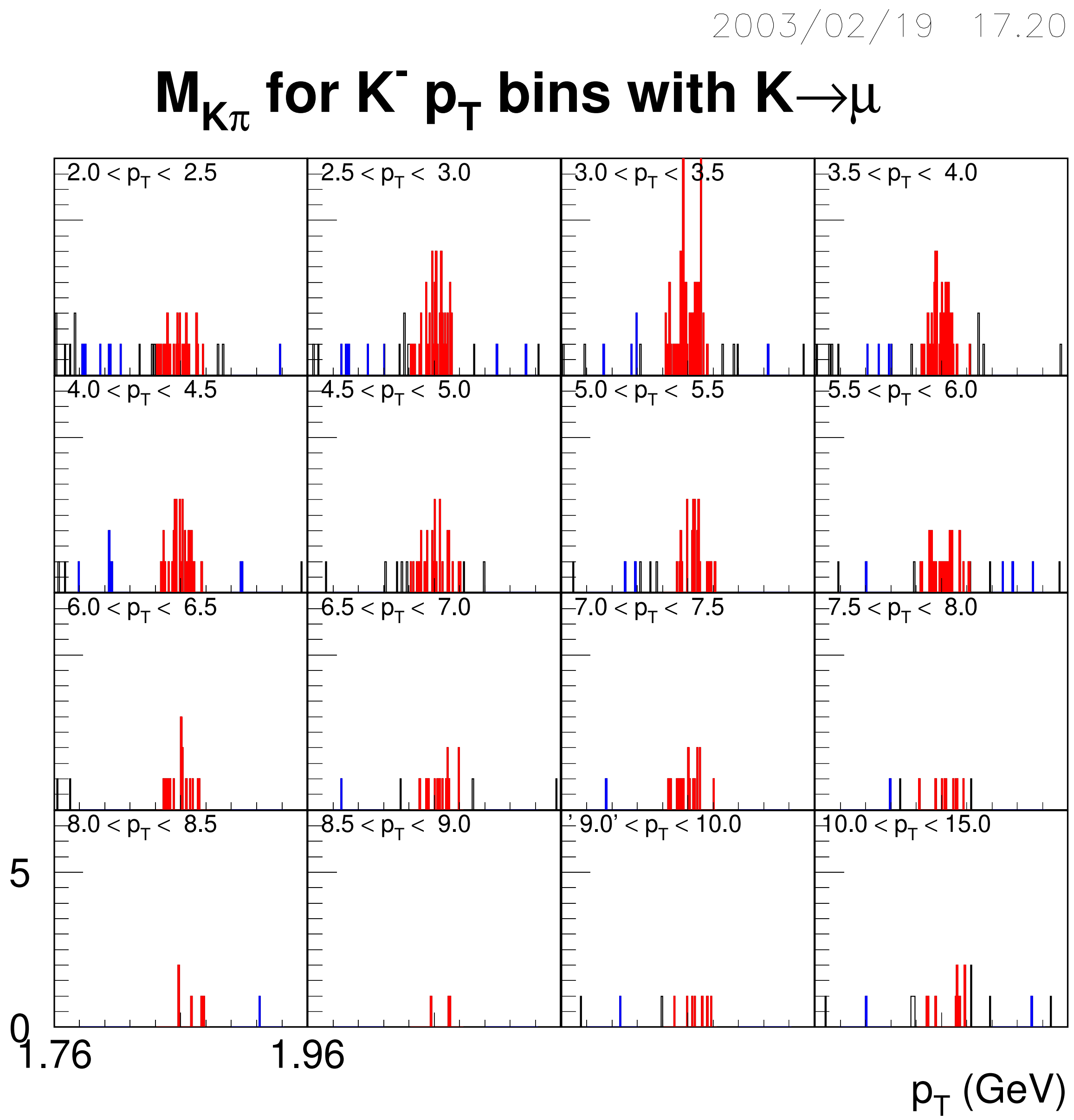

Figure 22: $K^-\pi^+$ mass spectra for kaons matched to a muon stub, binned by p_T of the kaon.

(file = pi_misid.eps)

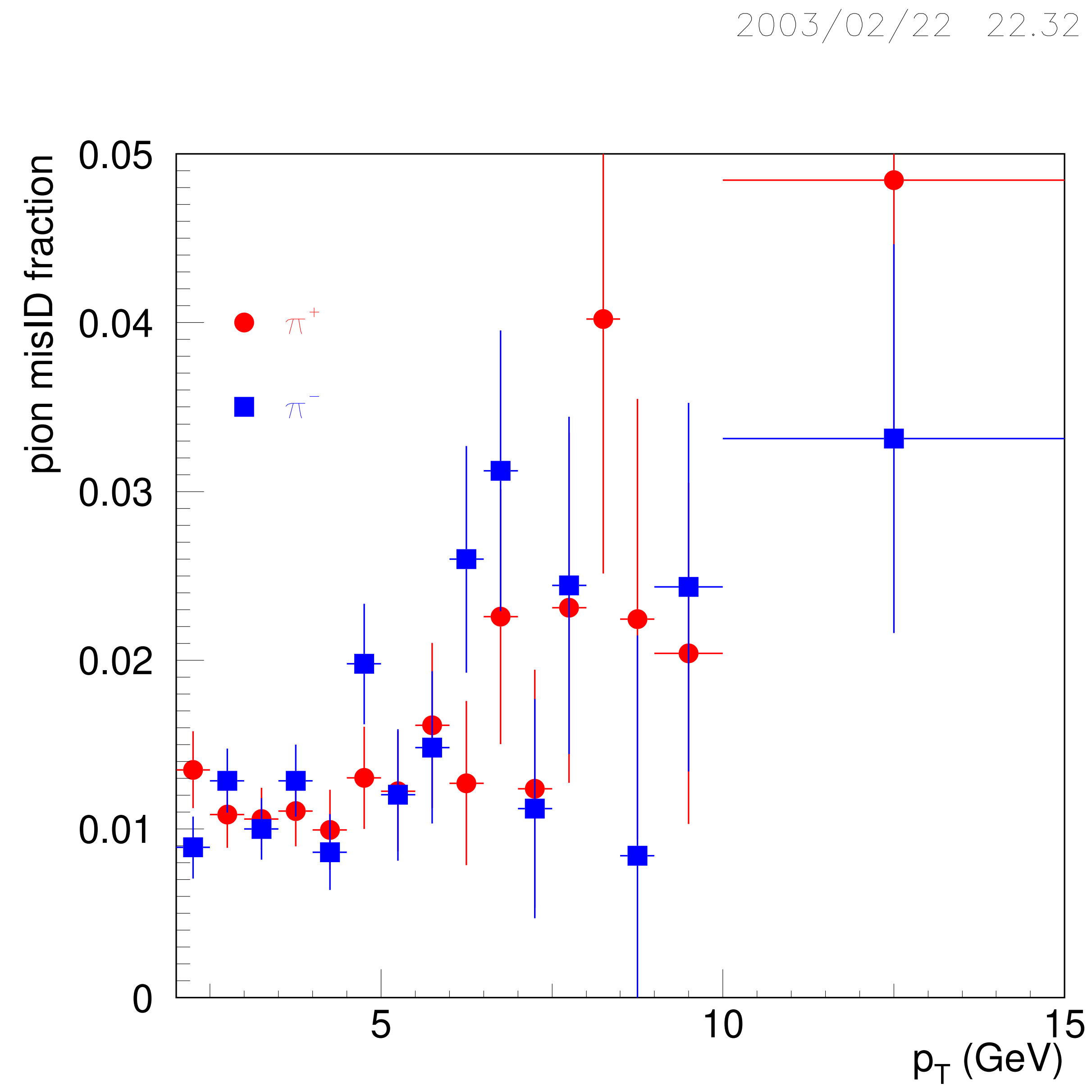

Figure 23: The fraction of $\pi^{\pm}$ misidentified as muons.

(file = k_misid.eps)

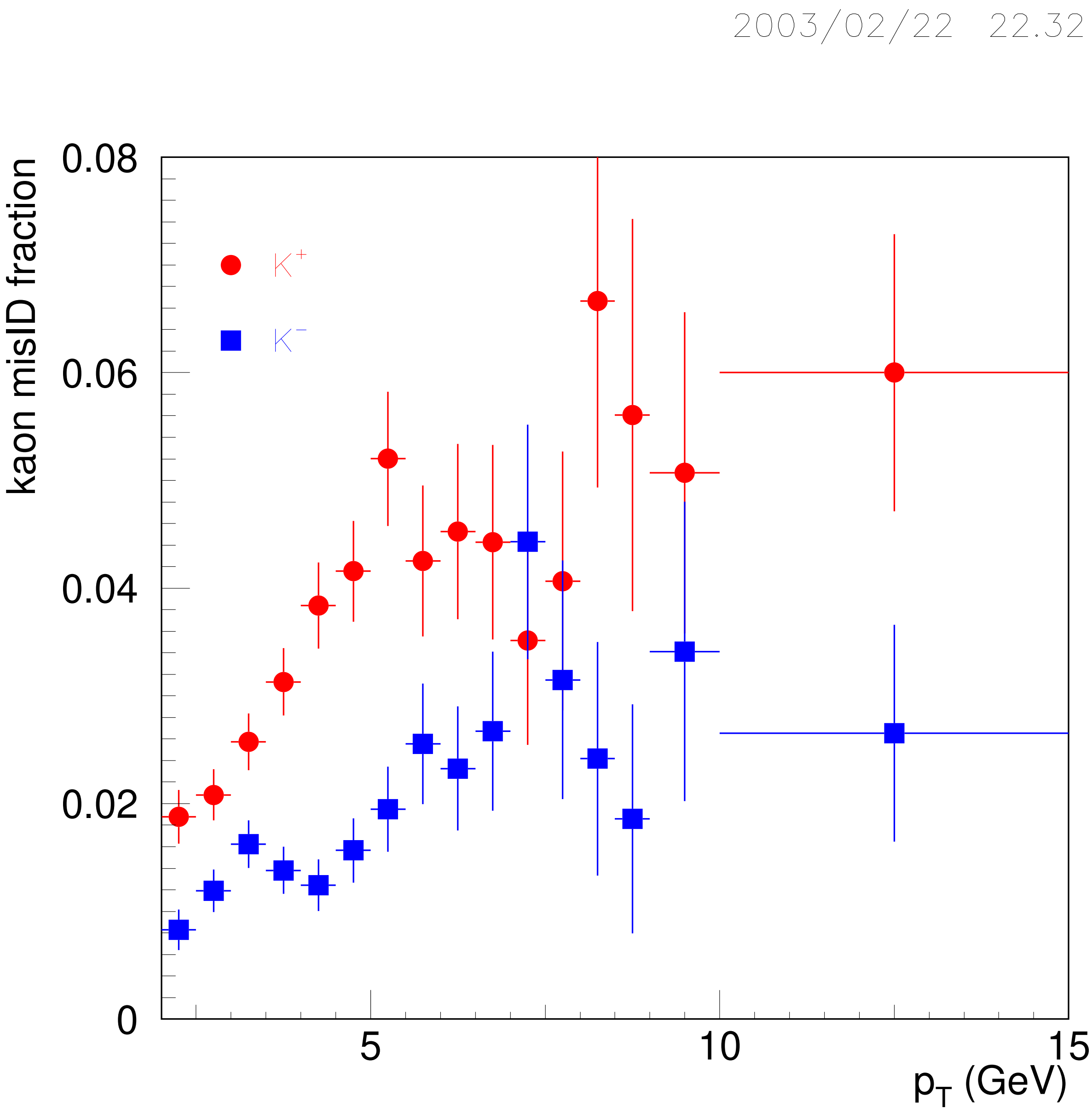

Figure 24: The fraction of $K^\pm$ misidentified as muons.

p_T range	π^+	π^-	K^+	K^-
2.0 to 2.5	1.35 ± 0.23	0.89 ± 0.18	1.88 ± 0.25	0.83 ± 0.19
2.5 to 3.0	1.09 ± 0.20	1.29 ± 0.19	2.08 ± 0.24	1.19 ± 0.20
3.0 to 3.5	1.06 ± 0.18	1.00 ± 0.18	2.57 ± 0.26	1.62 ± 0.22
3.5 to 4.0	1.11 ± 0.21	1.29 ± 0.21	3.13 ± 0.31	1.38 ± 0.22
4.0 to 4.5	0.99 ± 0.24	0.86 ± 0.22	3.84 ± 0.40	1.24 ± 0.24
4.5 to 5.0	1.30 ± 0.30	1.98 ± 0.36	4.16 ± 0.47	1.57 ± 0.30
5.0 to 5.5	1.22 ± 0.36	1.20 ± 0.39	5.20 ± 0.62	1.95 ± 0.40
5.5 to 6.0	1.61 ± 0.49	1.48 ± 0.45	4.25 ± 0.70	2.56 ± 0.56
6.0 to 6.5	1.27 ± 0.49	2.60 ± 0.67	4.53 ± 0.82	2.33 ± 0.57
6.5 to 7.0	2.26 ± 0.76	3.12 ± 0.83	4.43 ± 0.90	2.67 ± 0.74
7.0 to 7.5	1.24 ± 0.71	1.12 ± 0.65	3.51 ± 0.97	4.43 ± 1.09
7.5 to 8.0	2.31 ± 1.04	2.44 ± 1.00	4.07 ± 1.20	3.15 ± 1.11
8.0 to 8.5	4.02 ± 1.51	0.00 ± 0.26	6.67 ± 1.73	2.42 ± 1.08
8.5 to 9.0	2.24 ± 1.30	0.84 ± 1.31	5.61 ± 1.82	1.86 ± 1.06
9.0 to 10.0	2.04 ± 1.01	2.43 ± 1.09	5.07 ± 1.49	3.41 ± 1.39
10.0 to 15.0	4.85 ± 1.52	3.31 ± 1.15	6.00 ± 1.29	2.65 ± 1.01

Table 1: Probability (in percent) to misidentify a $\pi^\pm$ or $K^\pm$ as a muon for the p_T bins listed.

a total double-tagged background of $(1330 + 440) \times 0.014^2 = 0.35$ events. In practice, we will find that this naive estimate is a bit too optimistic. Read on ...

Fortunately, we have at least two potential handles on each of the two background components. For the resonant background, we can look at either double-tagged $K\pi$ events or single-tagged $\pi\pi$ events.[10] For the combinatorial background, we can look at the high-mass $\pi\pi$ sideband with a double tag, the high-mass $\pi\pi$ sideband with a single tag, and possibly the double-tagged $K\pi$ sidebands. Having multiple handles allows us to use one handle for tuning the cuts and another for extracting a final background estimate.

We look first at the double-tagged $K\pi$ peak. Ignoring sideband subtraction, there are 39791 $K\pi$ events in the region of figure 10 (lower) from 1.840 to 1.885 GeV. Of these, 1494 have exactly one muon tag, and 49 have two muon tags. Ignoring the $(1-p)$ in $2p(1-p)$, we expect $(0.024 + 0.014) \times 39791 = 1512$ single tags (this agrees basically by construction) and $0.024 \times 0.014 \times 39791 = 13$ double tags. The rate of double tags is alarmingly higher than the naive estimate—by a factor 3.8 ± 1.1.

Next, we look at the single-tagged $\pi\pi$ peak. After a crude sideband subtraction, there are 38 ± 10 single-tagged events out of 1583 total, for a pion fake rate of $38/1583/2 = 1.2 \pm 0.3\%$, consistent with the expected 1.4%.

In the high-mass $\pi\pi$ sideband, $1.90 < m_{\mu\mu} < 2.05$ GeV, there are 558 events before tagging, 47 with a single tag, and 7 with two tags. The track tag rate is $47/558/2 = 4.2\%$, larger than the kaon fake rate, perhaps implying that some real muons lurk in the sidebands. If the tracks are tagged independently, the double-tag count should be $558 \times 0.042^2 = 1$, but we see 7 events!

If our understanding of the backgrounds stopped here, we might expect $3.8 \times 0.35 + 7 \times \frac{44}{150} = 3.4$ background events in our search window—not a great place to be. We search for cuts to reduce these backgrounds and correlations.

A hand-scan of double-tagged $K\pi$ events reveals that there are many cases in which the two candidate tracks extrapolate to nearly the same location in the CMU. We construct a ϕ_{CMU} variable by extrapolating the track as a helix out to the solenoid radius $r = 144$ cm, and then as a straight line to the CMU, $r \approx 347$ cm. Note that the right thing to do would be to check `CdfMuon::trackPosition(CMU)` or `MuonStub::spacePoint()`, but doing so at this point would require re-running over the entire `B_CHARM` sample with the muon reconstruction module in front of the analysis module. Note also that the B field outside of the solenoid is not zero. We tried using -6% of the solenoidal field, but it gave worse results than the straight-line extrapolation. Figure 25 shows that about half of double tags, but only about 10–15% of pairs overall, have $\Delta\phi < 100$ mrad. This looks like a cut worth optimizing.

(10) Here, single-tagged means that both tracks are fiducial and there is one and only one tag, so that even a large $\mu\mu$ signal will make a negligible contribution.

$(\texttt{file} = \texttt{dphicmu.ps})$

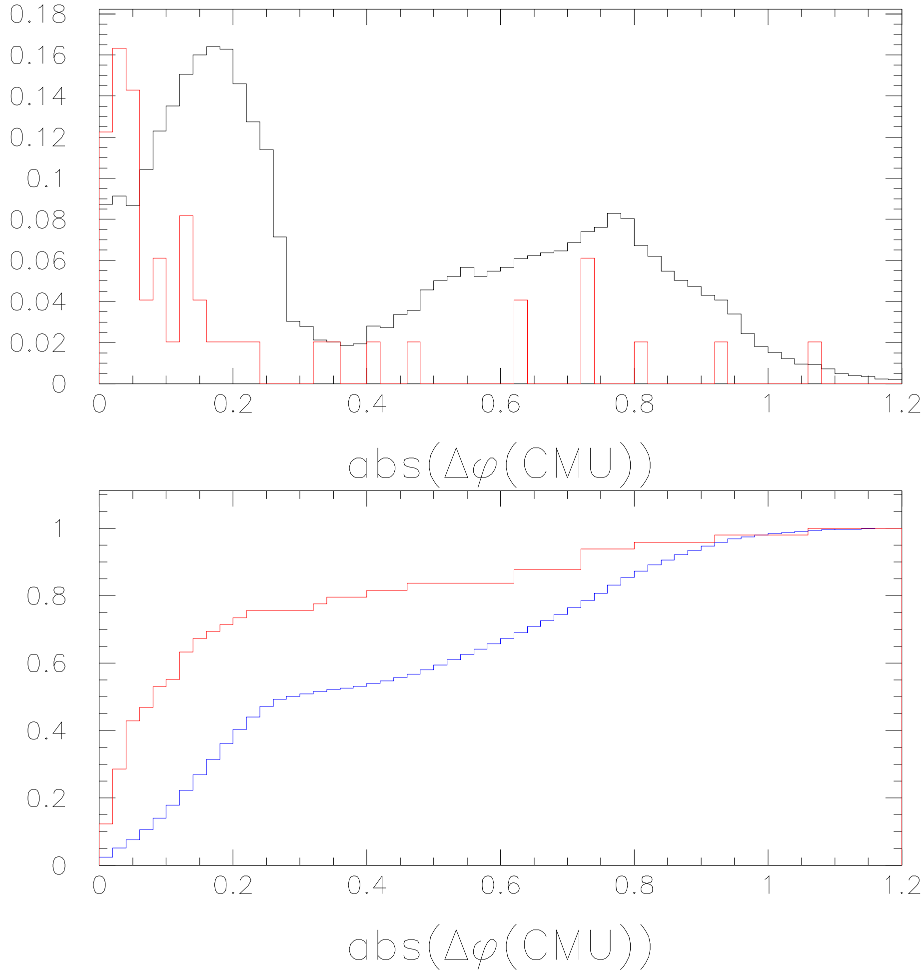

Figure 25: Distance (in radians, with approximate swimming) between $D^0 \to K\pi$ daughter tracks. The double-tagged pairs are shown in red. The black/blue curves are untagged pairs. The lower plot shows the integral distributions.

If track pairs from combinatorial background result from random overlap, then they should be less likely to point back at the beamline than real (primary) D^0 candidates. In addition, D^0's that come from B decay are more likely to be accompanied by real leptons than primary D^0's. See figure 26. This, too, looks like a cut worth optimizing.

Empirically, track pairs from the combinatorial background tend toward somewhat higher L_{xy} than track pairs from the $D^0 \to K\pi$ peak. We are not sure why. See figure 27. It also seems plausible that D^0's from B decay, which are likely to have real leptons nearby, decay farther from the origin. So we look for an optimal cut on this variable, too.

Finally, B decay and gluon splitting to $c\bar{c}$, both likely to produce nearby leptons, seem likely to produce other nearby tracks. In addition, many of the double-tagged $K\pi$ candidates are unusually busy events. An isolation cut on the D^0 ought to clean this up. See figure 28. We define isolation as $\frac{p_T(D^0)}{\sum p_T(\Delta R<0.25)}$, summing over all tracks of $p_T > 0.4$ GeV in the cone.

There are other cuts we haven't tried yet. One idea is to require a CMP stub for the tracks that are CMP fiducial and are of sufficient momentum to reach the CMP (if they're muons). This is particularly important because the punch-through rate increases with momentum. Another idea (thanks to TJL) is to cut on the CMU slope match to clean up poorly matched muon candidates. We aim to try these ASAP.

Now that we've chosen a few promising clean-up variables, we need a way to choose optimal cuts.

Giovanni Punzi has argued [7] that a reasonable definition of sensitivity in a counting experiment searching for a new process of unknown branching ratio is the range of branching ratios that one's search can discover at $\alpha\sigma$ significance. Applying this definition to Poission statistics, he derives the approximate figure of merit $S/(\alpha + 2\sqrt{B})$. Plugging in $\alpha = 3$, this is proportional to $S/(1.5 + \sqrt{B})$. This expression has the nice feature that it reduces to the usual $S/\sqrt{B}$ when the background rate is large and to S (times a constant) when the background rate is negligible compared to the smallest possible Poisson upper limit on the number of observed events (e.g. 2.3, 3.0, etc. for no observed events). Hence, we will seek selection criteria that maximize $\epsilon_{D^0\to\mu\mu}/(1.5 + \sqrt{B})$, where $\epsilon_{D^0\to\mu\mu}$ is signal efficiency and B is the expected number of background events.

To use this figure of merit, we need something proportional to signal efficiency (such as the area of the $D^0 \to \pi\pi$ normalization peak) and a properly normalized estimate of expected background.

As a starting point, and for cut optimization, we will use the double-tagged $K\pi$ signal (scaled down by the ratio of pions' to kaons' rates to fake muons) and the single-tagged $\pi\pi$ high-mass sideband. For this optimization, we take the sideband

(`file` = `dd0.ps`)

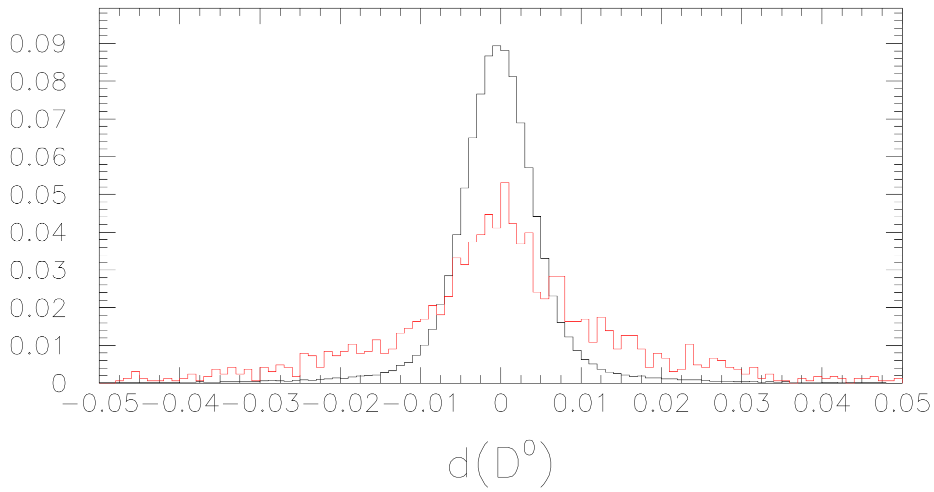

Figure 26: Impact parameter of the D^0 pseudotrack. $D^0 \to K\pi$ is shown in black. The high-mass $\pi\pi$ sideband is shown in red. Both curves are normalized to unit area.

(file = lxy.ps)

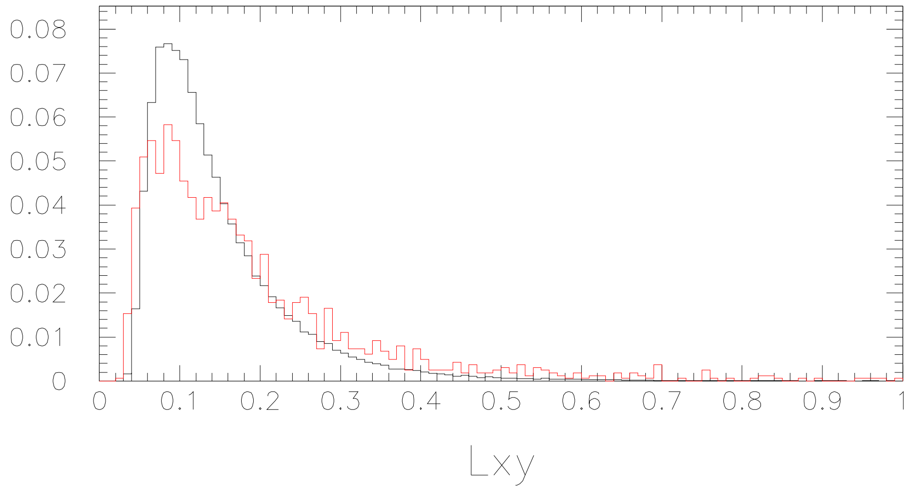

Figure 27: Decay length of the D^0. $D^0 \to K\pi$ is shown in black. The high-mass $\pi\pi$ sideband is shown in red. Both curves are normalized to unit area.

(file = isol.ps)

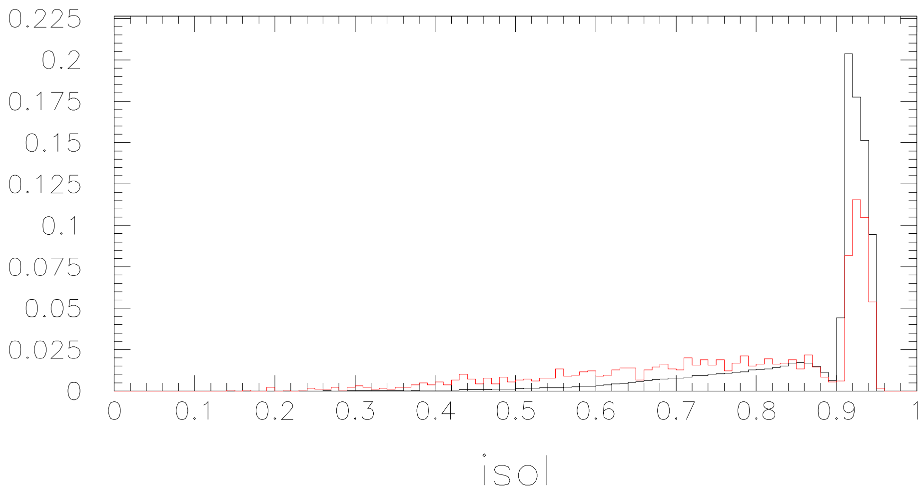

Figure 28: Decay length of the D^0. $D^0 \to K\pi$ is shown in black. The high-mass $\pi\pi$ sideband is shown in red. Both curves are normalized to unit area.

double-tag rate to be four times the uncorrelated rate.

We optimize the four cut variables: $|d_{D^0}|$, $|\Delta\phi_{\mathrm{CMU}}|$, L_{xy}, and I. Table 2 shows the results of the optimization. The precise cut values were optimized before we included the good run list; in the meantime, the isolation cut seems no longer to be a winner, for any cut value, so we drop it.

Cut	S	$\pi\pi$	comb	BG	FOM
`.true.`	1586	1.28	1.06	2.33	524
$\lvert d_{xy}\rvert < 0.0150$ cm	1534	1.15	0.80	1.95	529
$\lvert\Delta\phi_{\mathrm{CMU}}\rvert > 0.085$	1452	0.63	0.77	1.40	542
$L_{xy} < 0.45$ cm	1573	1.05	1.02	2.07	535
all but L_{xy}	1401	0.60	0.49	1.09	550
all but $\lvert\Delta\phi_{\mathrm{CMU}}\rvert$	1536	1.00	0.73	1.73	545
all but d_{xy}	1446	0.55	0.77	1.32	546
all	1409	0.53	0.47	0.99	564

Table 2: Cut optimization results.

We estimate the final combinatoric background in the search window using a high mass sideband covering the 150 MeV wide dimuon mass interval from 1.90 GeV to 2.05 GeV. Scaling the number of double-tag sideband events by the relative sizes of the search window and sideband window yields an estimate of

$$n_{\mathrm{comb.bkg.}} = (5 \pm \sqrt{5})\frac{44\,\mathrm{MeV}}{150\,\mathrm{MeV}} = 1.5 \pm 0.7 \text{ events.} \tag{7.1}$$

Going back to the $K\pi$ peak after the final cuts, we find that 21/35000 candidates have double muon tags, compared with 12 expected from the products of the K, π fake rates. We then look at the $\pi\pi$ single-tagged peak. We fit 1429 ± 56 events after all cuts. Adding a single muon tag, we fit 22 ± 8 events. (See figure 29.) Dividing by two ($2p(1-p)$), multiplying by the 1.4% muon fake rate, and multiplying by two for the remaining correlation seen in the $K\pi$ sample, we get 0.3 ± 0.1 events.

So the total estimated background is 1.8 ± 0.7 events.

8 Closed-box sensitivity

The fit to the $\pi^+\pi^-$ signal, above, yields an estimate of $N(\pi\pi) = 1412 \pm 54$ events (Fig. 30) in our normalization mode integrated over the ± 22 MeV search window.

If no event is found, then the limit at 90% CL will be

$$1.4 \times 10^{-3} \;\times\; \frac{2.3}{1412} \times 1.13 \times 0.96 \;=\; 2.5 \times 10^{-6}. \tag{8.1}$$

(file = afteroptcuts.ps)

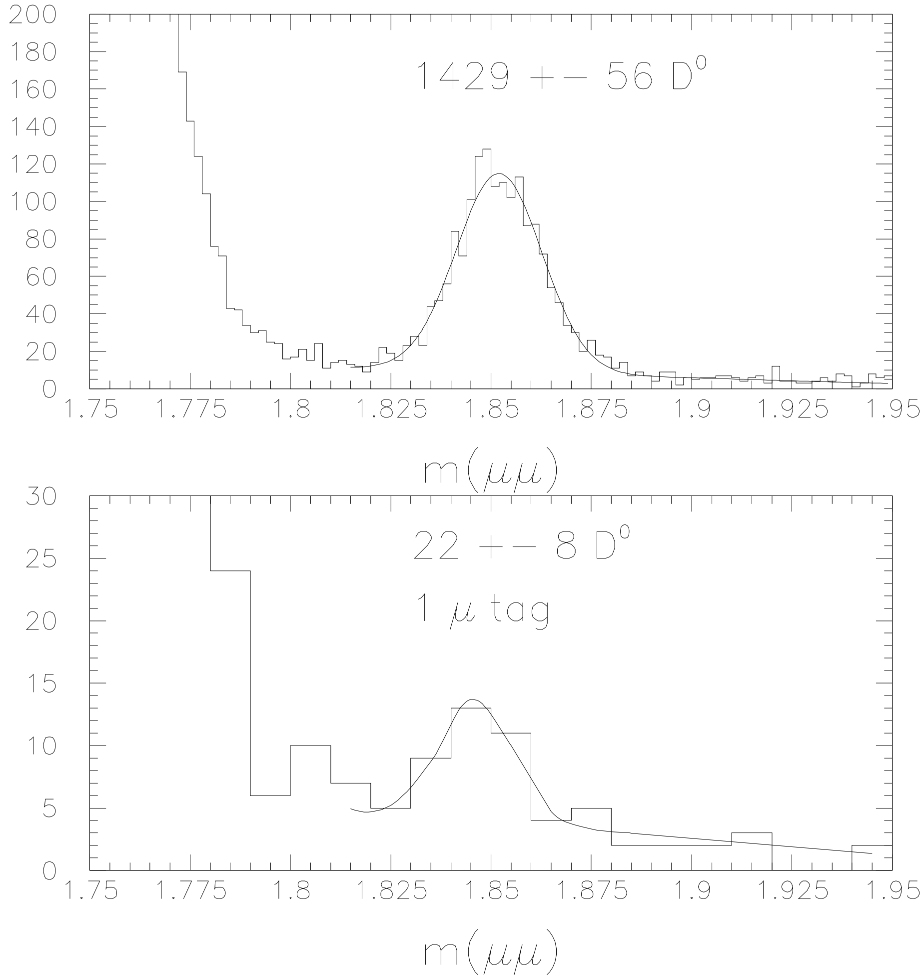

Figure 29: Mass spectra (using $\mu\mu$ hypothesis) after optimization cuts. Upper graph is without any muon tags. Lower graph is with exactly one muon tag.

(file = normalization.eps)

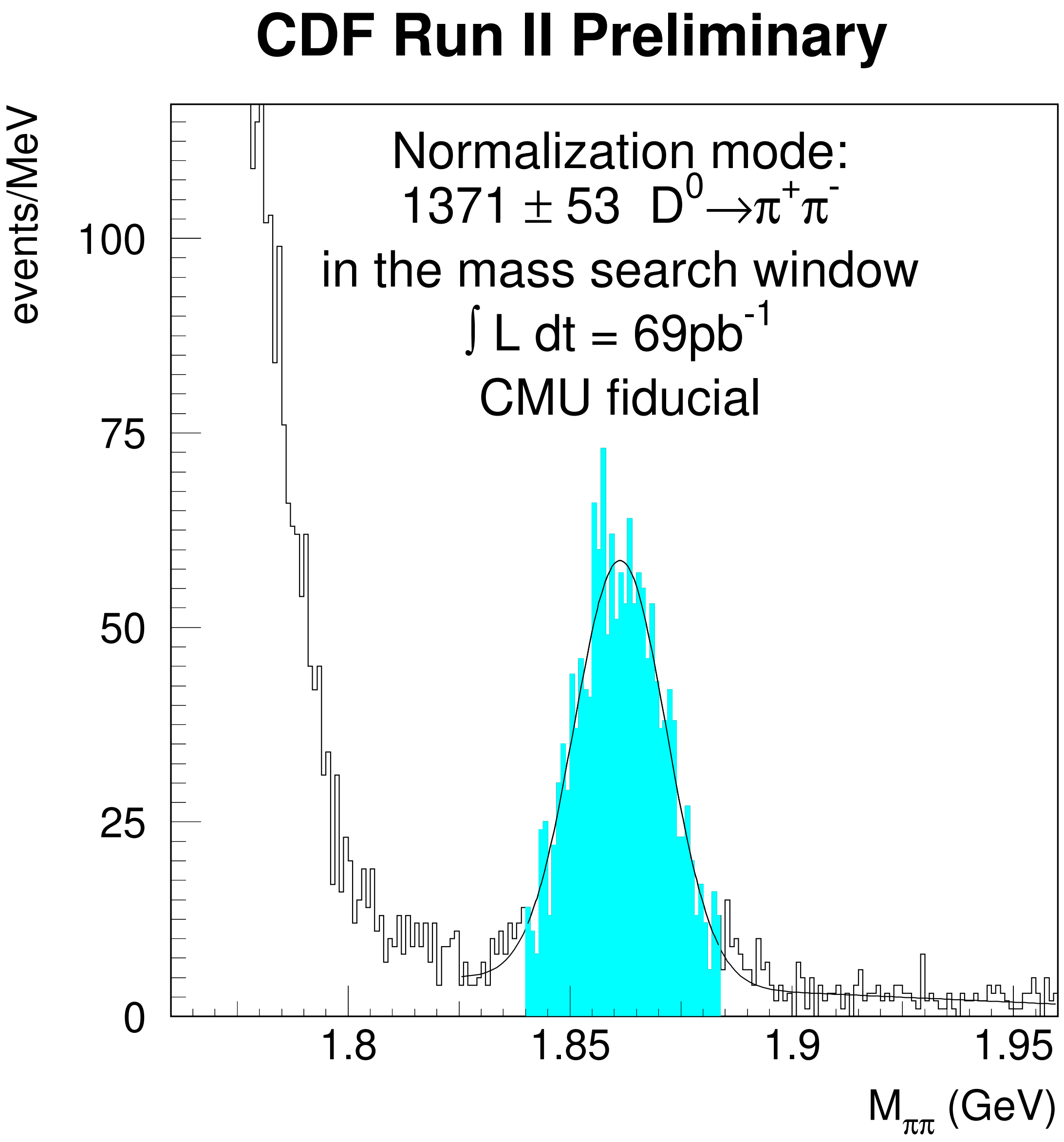

Figure 30: The mass spectrum of $D^0 \to \pi^+\pi^-$ candidates with $D^{*\pm}$ selection, and all analysis cuts. The peak is fit to a Gaussian signal plus linear background.

If we observe 2 events, the background estimate, then, using the procedure of Refs. [10] or [11] we would get

$$1.4 \times 10^{-3} \ \times \ \frac{4.0}{1412} \times 1.13 \times 0.96 \ = \ 4.3 \times 10^{-6}. \tag{8.2}$$

It is a bit disappointing that our final background estimate is 2 events, when we ought to have been able to reach ~ 0.5 events. Perhaps we should look harder in the coming week?

We could improve this by about a factor 1.5 by using CMX, and perhaps a similar factor by using the μ+SVT trigger. We disfavor the latter, because it fundamentally changes the analysis strategy, by requiring us to understand the relative efficiencies of two very different trigger paths. Nevertheless, it is reasonable to assume that with $\mathcal{O}(200 \text{ pb}^{-1})$ of good data on tape, CDF can reach the level of $\sim 2 \times 10^{-7}$ at which the $D^0 \to \pi^+\pi^-$ background becomes important.

8.1 Systematic uncertainties

The uncertainties in $\mathcal{B}(D^0 \to \pi^+\pi^-)$, $N(\pi\pi)$, $\epsilon(\pi\pi)/\epsilon(\mu\mu)$, and $a(\pi\pi)/a(\mu\mu)$ can be incorporated into the limit using the procedure of Cousins and Highland [12]. By recasting the equation, they derive an expression for a correction to $N^{\text{upper}}_{90\%\text{CL}}$ given by:

$$\Delta N^{\text{upper}}_{90\%\text{CL}} = \frac{1}{2}\left(N^{\text{upper}}_{90\%\text{CL0}}\right)^2 \left(\frac{\delta S}{S}\right)^2 \tag{8.3}$$

where $N^{\text{upper}}_{90\%\text{CL0}}$ is the limit on the number of signal events before systematic error correction, and

$$S = \frac{\mathcal{B}(D^0 \to \mu^+\mu^-)}{N(\pi\pi)} \frac{\epsilon(\pi\pi)}{\epsilon(\mu\mu)} \frac{a(\pi\pi)}{a(\mu\mu)}. \tag{8.4}$$

All of the uncertainties are less than 5% making the resulting correction negligible.

9 Opening the box

Before looking inside the box, we should be confident in the cut optimization procedure and the figure of merit used in the optimization. Then if we think of a new cut to apply to the coming months' data, we can use objective criteria to evaluate the cut, and we do not necessarily have to wait for a completely new, unbiased sample.

The B-Physics group agreed to opening the box and the result was presented at the March 13, 2003 B Physics meeting. When the the optimized cuts were applied, zero events survived in the search window (Fig. 31). We set an upper linit on the branching ratio of

$$\mathcal{B}(D^0 \to \mu^+\mu^-) \leq 2.5 \times 10^{-6} \tag{9.1}$$

at the 90% confidence level, and 3.3×10^{-6} at the 95% confidence level. As stated above, no systematic error correction is needed.

10 Work to do

Here is a list of things that we think we could do to improve this analysis or to document things we have learned while working on this analysis.

- Proof that muon detection is efficient, overall and run-by-run
- Graphs showing that XFT matching cuts are reasonable

Future directions:

- Rob wants to extend to $D^+ \to \pi^+\mu\mu$
- Bill wants to extend to $D^0 \to e\mu$ (and maybe ee)

11 Acknowledgements

B.A. would like to thank Marjorie Shapiro for suggesting this analysis topic in the year 2002 and Jay Hauser for suggesting it way back in 1996 (before we had the easy normalization signal).

References

[1] G. Burdman, E. Golowich, J. Hewett, S. Pakvasa, "Rare Charm Decays in the Standard Model and Beyond," hep-ph/0112235 v2 (March 2002).

[2] M. Adamovich *et al.* (BEATRICE Collaboration), "Search for the flavour-changing neutral-current decay $D^0 \to \mu^+\mu^-$," Phys. Lett. **B408**, 469 (1997).

[3] K. Hagiwara *et al.* (Particle Data Group), "Review of Particle Physics," Phys. Rev. **D66** 010001 (2002).

[4] A. Pompili (for the BaBar collaboration), "Charm Mixing and Lifetimes at Babar," hep-ex/0205071 (May 2002).

(file = result.eps)

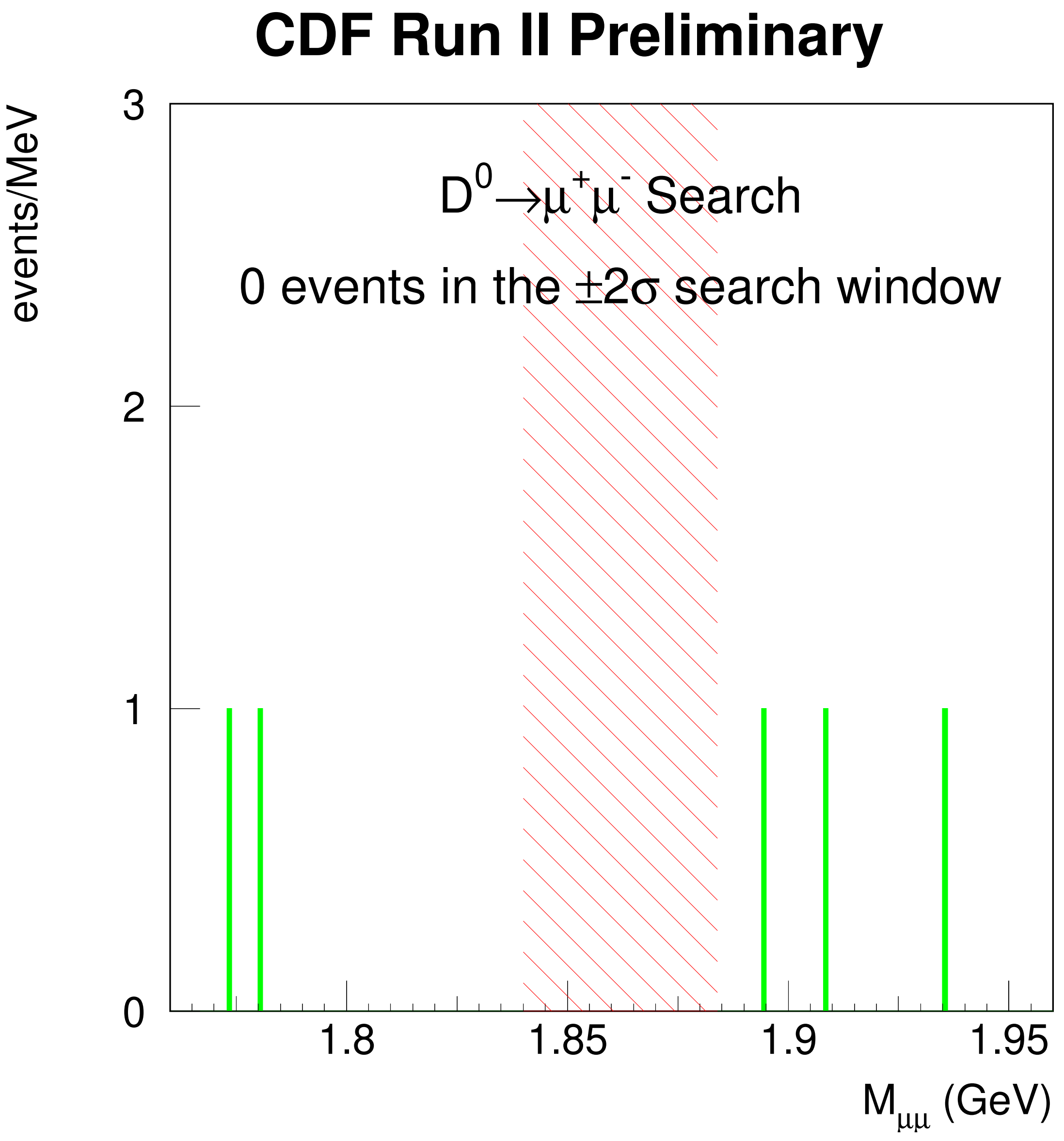

Figure 31: The mass spectrum of $\mu\mu$ events with $D^{*\pm}$ selection, all analysis cuts, and each track tagged as a muon. No events remain in the $D^0 \to \mu^+\mu^-$ search window.

[5] K. Senyo (for the Belle collaboration), "$B \to X_s \ell^+ \ell^-$ at Belle," hep-ex/0207005 (July 2002).

[6] A. Cerri, S. De Cecco, S. Giagu, M. Rescigno, "A Measurement of The Relative Branching Fractions: $BR(D^0 \to K\pi/KK/\pi\pi)$," CDF note 6018 (September 2002).

[7] G. Punzi, "Optimization of searches for new signals," presentation to CDF Statistics Committee (January 22, 2003), `http://www.pi.infn.it/~punzi/optimal_search.ppt` .

[8] K. Bloom, D. Dagenhart, "Muon-Reconstruction Efficiency," CDF note 6029 (July 2002).

[9] T. LeCompte, "Efficiency of Momentum Dependent Muon Matching Cuts," CDF note 6114 (September 2002).

[10] B.P. Roe and M.B. Woodroofe, Phys. Rev. **D63**, 013009 (2000).

[11] G.J. Feldman and R.D. Cousins, Phys. Rev. **D57**, 3873 (1998).

[12] R.D. Cousins and V.L. Highland, Nucl. Instrum. Meth. **A320**, 331 (1992).